CANADIAN THESES ON MICROFICHE

THÈSES CANADIENNES SUR MICROFICHE

National Library of Canada
Collections Development Branch

Canadian Theses on
Microfiche Service

Ottawa, Canada
K1A 0N4

Bibliothèque nationale du Canada
Direction du développement des collections

Service des thèses canadiennes
sur microfiche

NOTICE

The quality of this microfiche is heavily dependent upon the quality of the original thesis submitted for microfilming. Every effort has been made to ensure the highest quality of reproduction possible.

If pages are missing, contact the university which granted the degree.

Some pages may have indistinct print especially if the original pages were typed with a poor typewriter ribbon or if the university sent us an inferior photocopy.

Previously copyrighted materials (journal articles, published tests, etc.) are not filmed.

Reproduction in full or in part of this film is governed by the Canadian Copyright Act, R.S.C. 1970, c. C-30. Please read the authorization forms which accompany this thesis.

AVIS

La qualité de cette microfiche dépend grandement de la qualité de la thèse soumise au microfilmage. Nous avons tout fait pour assurer une qualité supérieure de reproduction.

S'il manque des pages, veuillez communiquer avec l'université qui a conféré le grade.

La qualité d'impression de certaines pages peut laisser à désirer, surtout si les pages originales ont été dactylographiées à l'aide d'un ruban usé ou si l'université nous a fait parvenir une photocopie de qualité inférieure.

Les documents qui font déjà l'objet d'un droit d'auteur (articles de revue, examens publiés, etc.) ne sont pas microfilmés.

La reproduction, même partielle, de ce microfilm est soumise à la Loi canadienne sur le droit d'auteur, SRC 1970, c. C-30. Veuillez prendre connaissance des formules d'autorisation qui accompagnent cette thèse.

THIS DISSERTATION
HAS BEEN MICROFILMED
EXACTLY AS RECEIVED

LA THÈSE A ÉTÉ
MICROFILMÉE TELLE QUE
NOUS L'AVONS REÇUE

Canada

NL 339 (r. 86/09)

70

0-315-21265-9

National Library of Canada | Bibliothèque nationale du Canada

Canadian Theses Division | Division des thèses canadiennes

Ottawa, Canada
K1A 0N4

PERMISSION TO MICROFILM — AUTORISATION DE MICROFILMER

• Please print or type — Écrire en lettres moulées ou dactylographier

Full Name of Author — Nom complet de l'auteur

DAVID ROSS RICKETTS

Date of Birth — Date de naissance

AUGUST 16, 1958

Country of Birth — Lieu de naissance

CANADA

Permanent Address — Résidence fixe

APT. 208 282 BROOKSIDE TERRACE
EDMONTON ALBERTA
T6H 4J6

Title of Thesis — Titre de la thèse

ULTIMATE BEHAVIOUR OF CONTINUOUS DEEP REINFORCED CONCRETE BEAMS

University — Université

UNIVERSITY OF ALBERTA

Degree for which thesis was presented — Grade pour lequel cette thèse fut présentée

MASTER OF SCIENCE

Year this degree conferred — Année d'obtention de ce grade

1985

Name of Supervisor — Nom du directeur de thèse

DR. J.G. MacGREGOR

Permission is hereby granted to the NATIONAL LIBRARY OF CANADA to microfilm this thesis and to lend or sell copies of the film.

The author reserves other publication rights, and neither the thesis nor extensive extracts from it may be printed or otherwise reproduced without the author's written permission.

L'autorisation est, par la présente, accordée à la BIBLIOTHÈQUE NATIONALE DU CANADA de microfilmer cette thèse et de prêter ou de vendre des exemplaires du film.

L'auteur se réserve les autres droits de publication; ni la thèse ni de longs extraits de celle-ci ne doivent être imprimés ou autrement reproduits sans l'autorisation écrite de l'auteur.

Date

Jan 3/85

Signature

David R Ricketts

NL-91 (4/77)

THE UNIVERSITY OF ALBERTA

ULTIMATE BEHAVIOUR OF CONTINUOUS DEEP REINFORCED CONCRETE BEAMS

by

DAVID R. RICKETTS

A THESIS

SUBMITTED TO THE FACULTY OF GRADUATE STUDIES AND RESEARCH

IN PARTIAL FULFILMENT OF THE REQUIREMENTS FOR THE DEGREE

OF MASTER OF SCIENCE

DEPARTMENT OF CIVIL ENGINEERING

EDMONTON, ALBERTA

SPRING 1985

THE UNIVERSITY OF ALBERTA

RELEASE FORM

NAME OF AUTHOR DAVID R. RICKETTS

TITLE OF THESIS ULTIMATE BEHAVIOUR OF CONTINUOUS DEEP REINFORCED CONCRETE BEAMS

DEGREE FOR WHICH THESIS WAS PRESENTED MASTER OF SCIENCE

YEAR THIS DEGREE GRANTED SPRING 1985

Permission is hereby granted to THE UNIVERSITY OF ALBERTA LIBRARY to reproduce single copies of this thesis and to lend or sell such copies for private, scholarly or scientific research purposes only.

The author reserves other publication rights, and neither the thesis nor extensive extracts from it may be printed or otherwise reproduced without the author's written permission.

(SIGNED) David R. Ricketts

PERMANENT ADDRESS:

208 - 282 Brookside Terrace

Edmonton, Alberta

T6H 4J6

DATED Dec. 12/84

THE UNIVERSITY OF ALBERTA

FACULTY OF GRADUATE STUDIES AND RESEARCH

The undersigned certify that they have read, and recommend to the Faculty of Graduate Studies and Research, for acceptance, a thesis entitled ULTIMATE BEHAVIOUR OF CONTINUOUS DEEP REINFORCED CONCRETE BEAMS submitted by DAVID R. RICKETTS in partial fulfilment of the requirements for the degree of MASTER OF SCIENCE.

.....

Supervisor

.....

.....

Date.....Dec 12/84.....

ABSTRACT

This research study was designed to be a continuation of a more general study of deep beam behaviour carried out at the University of Alberta (Rogowsky 1983).

The current study explores three aspects of deep beam behaviour using a plastic truss model which has been proposed to explain the behaviour of deep beams:

1. The ability of deep beams containing light vertical web reinforcement to fully develop the stress field suggested by the model. This involved the testing of one, two span continuous beam.
2. The change in shear strength, v_u/f_c', with a change in the span to depth ratio, a/d, for beams with heavy vertical web reinforcement. This involved the testing of one two span continuous beam.
3. The flexibility of the plastic truss model to account for varying distributions of top and bottom chord steel in continuous deep beams. This involved the testing of three; two span continuous deep beams with a medium amount of vertical web steel. Two of these beams had top and bottom chord steel distributions which were significantly different from the distribution suggested by the elastic bending moments.

The five beams tested as part of this study had an a/d ratio of approximately 0.79. The beams were loaded and supported with columns cast monolithically with the beams.

Generally the failure of the beams was initiated by yielding of some of the reinforcing steel, followed by crushing of the concrete struts near the load or support columns. All of the beams failed at a load very close to the values predicted by the plastic truss model.

In the case of the beam with light vertical web steel, the bottom chord and stirrups did yield while the top chord did not, indicating that the full plastic redistribution of forces was not achieved. The failure to redistribute forces in this beam can be attributed to a lack of overall stiffness in the interior web members.

The beam with heavy vertical web steel failed at a load corresponding to a high shear strength, v_u/f'_c, indicating that it was possible to increase shear strength with an increase in vertical web reinforcement.

The final three beams all failed after both the top and bottom chords had yielded. This finding suggests that the plastic truss model is flexible with regards to the distribution of top and bottom chord steel areas.

ACKNOWLEDGEMENTS

The guidance and counsel provided by Professor J. G. MacGregor during the course of this project are greatly appreciated.

I would also like to express my gratitude for the assistance and cooperation of the technical staff of the I. F. Morrison Structural Labratory; Larry Burden, Richard Helfrich and Vijay Parmar. In particular I would like to thank Richard Helfrich for his initiative in carrying out the construction of the specimens and in the setting up of the test apparatus.

My thanks are also extended to Dr. B. Thürlimann for his advice on the area of reinforced concrete plasticity.

The financial support for this project provided by the Natural Science and Engineering Research Council of Canada (NSERC) and Morrison Hershfield Ltd. is also appreciated.

Finally, I am grateful to my wife, Nancy for her support and encouragement throughout this project. Her assistance and understanding during the long and inconvenient hours made possible the completion of this study.

Table of Contents

Chapter		Page
1.	INTRODUCTION	1
	1.1 General	1
	1.2 Objectives	2
	1.3 Outline	4
2.	THEORETICAL BACKGROUND	5
	2.1 General	5
	2.2 Plastic Truss Model	5
	2.2.1 General Features	5
	2.2.2 Effective Concrete Strength	8
	2.3 Advanced Stress Fields	11
3.	EXPERIMENTAL PROGRAM	12
	3.1 Test Specimens	12
	3.1.1 Introduction	12
	3.1.2 Selection of Variables in Test Program	13
	3.1.3 Details of Specimens	14
	3.2 Materials	21
	3.2.1 Reinforcing Steel	21
	3.2.1.1 Steel Properties	21
	3.2.1.2 Assembly	23
	3.2.2 Concrete	27
	3.3 Instrumentation	29
	3.3.1 General	29
	3.3.2 Loads and Reactions	31
	3.3.3 Strains	31
	3.3.4 Displacements	34

3.4 Testing 35
3.4.1 Test Set-Up 35
3.4.2 Test Procedure 35
4. TEST RESULTS 38
4.1 Presentation of Results 38
4.2 Failure Loads 38
4.3 Deflections 40
4.4 Results of Individual Beam Tests 42
4.4.1 Beam 1 42
4.4.2 Beam 2 47
4.4.3 Beam 3 48
4.4.4 Beam 4 52
4.4.5 Beam 5 56
5. INTERPRETATION OF TEST RESULTS 64
5.1 Truss Models 64
5.2 Calculation of the Effective Concrete Strength from the State of Strain in the Web 72
5.3 Ultimate Shear Strengths 78
5.4 Distribution of Reactions 82
5.5 Flexibility of Plastic Truss Model 82
6. SUMMARY AND CONCLUSIONS 87
REFERENCES 89

List of Tables

Table		Page
3.1	Reinforcing Steel Details	15
3.2	Reinforcing Steel Properties	24
3.3	Concrete Mix Design	28
3.4	Concrete Properties	30
4.1	Failure Loads, Reactions and Shear Strengths	39
5.1	Effectiveness Factor Calculated from the State of Strain	75
5.2	Ultimate Shear Strengths	79
5.3	Distribution of Reactions at Failure	83

List of Figures

Figure		Page
3.1	Beam 1: Dimensions and Details	16
3.2	Beam 2: Dimensions and Details	17
3.3	Beam 3: Dimensions and Details	18
3.4	Beam 4: Dimensions and Details	19
3.5	Beam 5: Dimensions and Details	20
3.6	20M Steel: Load-Deformation Curves	25
3.7	10M and 6 mm Steel: Load-Deformation Curves	26
3.8	Concrete Demec Target Layout	33
3.9	Test Frame and Set-Up	36
4.1	Load Deflection Curves	41
4.2	Beam 1: Crack Pattern	44
4.3	Beam 1: Concrete Compressive Strains	45
4.4	Beam 1: Steel Strains	46
4.5	Beam 2: Crack Pattern	49
4.6	Beam 2: Concrete Compressive Strains	50
4.7	Beam 2: Steel Strains	51
4.8	Beam 3: Crack Pattern	53
4.9	Beam 3: Concrete Compressive Strains	54
4.10	Beam 3: Steel Strains	55
4.11	Beam 4: Crack Pattern	57
4.12	Beam 4: Concrete Compressive Strains	58
4.13	Beam 4: Steel Strains	59
4.14	Beam 5: Crack Pattern	61
4.15	Beam 5: Concrete Compressive Strains	62

Figure Page

4.16 Beam 5: Steel Strains 63

5.1 Beam 1: Stress Field 65

5.2 Beam 2: Stress Field 66

5.3 Beam 3: Stress Field 67

5.4 Beam 4: Stress Field 68

5.5 Beam 5: Stress Field 69

5.6 Beam 1: Concrete Strains 73

5.7 Grid A: Mohr's Strain Circles 76

5.8 Grid B: Mohr's Strain Circles 77

5.9 Effect of Quantity of Vertical Web Reinforcement 81

List of Symbols

a = Shear span measured from the face of the load to the face of the support, mm

$A_{s,b}$ = Area of longitudinal reinforcing steel in the bottom chord, mm^2

$A_{s,t}$ = Area of longitudinal reinforcing steel in top chord, mm^2

A_v = Area of vertical web reinforcing steel per metre length of beam, mm^2

b = Width of beam, mm

d = Effective depth of beam, mm

E_c = Modulus of Elasticity for concrete, MPa

E_s = Modulus of Elasticity for steel, MPa

f'_c = Concrete compressive strength, MPa

f^*_c = Effective concrete compressive strength, MPa

f_t = Tensile strength of concrete as determined from a split cylinder test, MPa

f_y = Yield strength of reinforcing steel, MPa

P = Jack load, kN

R_1 = Exterior reaction, kN

R_2 = Interior reaction, kN

v_u = Ultimate shear stress at a section, V_u/bd, MPa

V_u = Ultimate shear at a section, kN

γ_{xy} = Shearing strain

ϵ_c = Compressive strain

ϵ_t = Tensile strain

ϵ_x = Longitudinal strain at mid-depth of the member

ϵ_1 = Principal tensile strain in cracked concrete

ϵ_{2m} = Principal concrete compressive strain corresponding to the highest point in a compressive stress-strain curve

θ = Angle of inclination of compression struts

ν = Concrete effectiveness factor, f_c^*/f_c'

ρ_v = Ratio of vertical web reinforcing steel area to effective concrete area, A_v/bd

σ_1 = Largest principal compressive stress in nodal area, MPa

σ_2 = Smallest principal compressive stress in nodal area, MPa

1. INTRODUCTION

1.1 General

Deep beams are beams in which the depth of the member is comparable to the span. These structural elements occur frequently as transfer girders, shear walls, coupling beams and pile caps. Several researchers have applied plasticity methods of analysis in explaining the behaviour of deep beams, including Thürlimann (1978; 1979), Nielsen (1978) and Marti (1978). Of particular relevance to the present study is the research conducted by Rogowsky (1983) at the University of Alberta. Rogowsky employed a plastic truss model to explain the behaviour of deep beams. The recent inclusion of a truss model in the 1984 Canadian Design Code for Concrete Structures (CSA Standard A23.3) would indicate that these models are gaining acceptance. Continued research into the applications of a plastic truss model is warranted, however, as there are still unanswered questions about this design method.

The present research study was designed to be a continuation of the general study undertaken by Rogowsky (1983). Rogowsky's work involved the testing of 23 beams, 6 of which were single spans and 17 of which were two span specimens. The primary variables in his series of tests were the shear span to depth ratio, a/d, and the orientation and quantity of web reinforcement. Rogowsky then utilized a plastic truss model to explain the behaviour of the 23

beams. Briefly, he concluded that a plastic truss model gave reasonable predictions of the mode of failure and the ultimate strengths, provided that an appropriate stress field was chosen to model the flow of forces in the beam.

Although Rogowsky's research provided an excellent introduction to an understanding of the behaviour of deep beams, there were some areas of deep beam behaviour which his test series did not fully explore and explain. The purpose of the present research study was to contribute to this knowledge base by exploring two particular aspects of Rogowsky's tests, and by investigating the flexibility of a plastic truss model in explaining the ultimate behaviour of deep beams.

1.2 Objectives

There were three specific objectives of this research project. The first and major objective was the investigation of the flexibility of a plastic truss model for continuous beams.

The truss model should give a lower bound solution for the ultimate load carrying capacity of the beam provided that, (i), the stress field satisfies equilibrium everywhere within the beam, and (ii), the stresses in the truss members do not exceed allowable stresses for the concrete and steel. It follows then, that the size of the truss members should be able to be arbitrarily varied and an appropriate stress field identified to predict ultimate behaviour. Rogowsky

(1983) varied the size of truss members by using different arrangements of web reinforcement. The current study varied the size of the top and bottom chords of the truss by varying the amounts of reinforcing steel in each chord. This involved the testing of three two-span continuous beams. By comparing the test results with the theoretical plastic trusses, or stress fields, it was possible to assess the flexibility of the model with respect to this parameter.

The second objective of this study was to further investigate one of Rogowsky's conclusions regarding the behaviour of deep beams. Rogowsky found that beams with heavy stirrup reinforcement did not exhibit a change in shear strength, v_u/f'_c, with a change in the shear span to depth ratio, a/d. Such a change would normally be associated with deep beam behaviour. The current study used a greater quantity of vertical web steel than that used in Rogowsky's tests in an attempt to increase the capacity of the beam beyond Rogowsky's values. This objective was achieved by testing one two-span continuous beam.

The final objective of this study was to further investigate one of Rogowsky's beams which did not behave as predicted by the plastic truss model; in particular, a beam in which the negative moment steel did not yield. Rogowsky offerred several possible explanations for the finding. The current study investigated the hypothesis that the detailing of the reinforcement in this beam may have prevented the redistribution of forces required to fully establish the

predicted stress field. One beam was tested which maintained all major parameters as in Rogowsky's beam 3/1.0, but which had two significant changes. This beam had increased cover to the longitudinal steel, and additional development length provided for the top chord steel in the area of the loading columns.

1.3 Outline

A review of the theoretical basis for the plastic truss model is presented in Chapter 2.

Chapter 3 outlines the objectives and the procedures followed in the experimental program. Included in this chapter are descriptions of the construction of the specimens, the experimental method, the instrumentation and the material tests.

The test series provided quantitative information on concrete strains, steel strains, deflections, loads and reactions, as well as qualitative observations of the behaviour of the beam. This information is summarized in Chapter 4.

Chapter 5 provides an interpretation of the test results based on predictions made using the plastic truss model.

A summary of the significant observations and conclusions is presented in Chapter 6.

2. THEORETICAL BACKGROUND

2.1 General

There has been considerable research conducted in the area of the behaviour of deep beams as well as the application of the theory of plasticity to reinforced concrete. The reader is referred to Chapter 2 of Rogowsky (1983) for a comprehensive review of this literature.

2.2 Plastic Truss Model

2.2.1 General Features

The lower bound theorem of plasticity states that if a distribution of stresses can be found that, (i), is in equilibirium with the applied load and, (ii), is at or below the strength of the material at every point in the structure, the structure will not collapse, or will just be at the point of collapse under the loads in question. Since the structure can carry at least this applied load, this distribution is a lower bound to the load carrying capacity of the structure. The plastic truss model used here utilizes this lower bound technique by idealizing the beam as a pin jointed truss with concrete struts acting as compression members and reinforcing steel acting as tension members. The analysis must ensure that no portion of the load path identified by the truss is overstressed.

There are several advantages to this approach. First, it should always provide a safe solution since it is a lower bound technique. It also represents the overall behaviour of the beam rather than just one stress component such as shear or bending moment. In addition, the truss model provides a visual interpretation of the flow of forces through the beam. One disadvantage of this approach is that it does not provide much information about the behaviour of the beam at service loads.

The application of the plastic truss model involves selecting a stress field which satisfies the following conditions and assumptions:

1. Equilibrium must be established.
2. Perfectly plastic behaviour of the concrete and steel is assumed. In the case of the steel, this implies that the elastic strains are negligible with respect to the post yield strains and that strain hardening of the steel is neglected. This is generally a safe and reasonable assumption. Strain softening of the concrete and the complex stress state often found in concrete truss members makes a similar assumption for the concrete not viable. In order to compensate for this non-ideal behaviour, an effectiveness factor, ν, is employed. This will be discussed in more detail later in this chapter. Thus the concrete will be assumed to resist compression only, and to have an effective compressive strength

$f_c^* = \nu f_c'$.

3. Steel is required to resist all tensile forces and is assumed to be at its yield stress at points of maximum stress in the bar.

4. The joints of the truss are accommodated through the use of 'hydrostatic stress' elements in which two of the principal stresses are equal to f_c^*. In fact these elements are not in a true hydrostatic state of stress because the out of plane stress will not equal f_c^*. This terminology is employed, however, since it is hydrostatic within the plane in which the forces are acting. To achieve this state of stress implies that all of the faces of the nodal element must be stressed to f_c^*. The concrete struts therefore, must be stressed to f_c^* where they meet the nodal element. The tension end anchorages of the bars must be able to positively anchor the bars and they must also spread the anchorage force over the depth of the nodal zone.

This hydrostatic behaviour is only possible at a joint if the centroid of each truss member coincides with the line of action of all external loads (i.e., there is no moment in the joint).

5. Failure of the truss occurs when a concrete compression member crushes or when sufficient steel tension members yield to form a mechanism. The yielding of the steel will not in itself result in a

failure but rather, will lead to increased straining. This in turn leads to excessive rotational straining in one of the joints and ultimately to failure of the concrete in the area of the joint.

2.2.2 Effective Concrete Strength

As indicated in the previous section, an effective concrete stress of $f_c^* = \nu f_c'$ is assumed to exist in the concrete elements of the truss. The determination of the effectiveness factor, ν, is the subject of much discussion within the plasticity literature. This factor must account for a number of variables which influence the stress state of each individual concrete element in the truss. The major effect accounted for by the effectiveness factor is the strain softening behaviour of the concrete in the struts due to cracking and transverse straining. This straining is due to the fact that the struts may be crossed by stirrups which are assumed to be stressed close to yield.

In the nodal zones the stress conditions are also complex. Strain incompatability between the tension steel anchored in such zones and the compressed concrete leads to the high local stesses adjacent to the bars in the concrete nodal areas. The magnitude of these stresses will vary depending on the concentration or spacing of the steel, and the concrete strains. The steel strain depends on the amount of vertical web steel and the amount of prestressing

introduced to the steel.

In addition, the degree of lateral confinement of the concrete in these nodal zones should play a major role in determining the effective concrete strength. Confinement by column reinforcement cages or adjacent floor slabs would be expected to increase the effective strength.

Due to the wide range of factors influencing the concrete strength in these areas, it is very difficult to quantify the effectiveness factor, ν, for all conditions.

Various authors have proposed different values for ν. Some have proposed values expressed in terms of cylinder strengths only:

Thurlimann (1976): $f_c^* = 0.6$ to $0.7f_c'$

CEB Model Code (1978), Refined Method: $f_c^* = 0.6f_c'$

M. P. Nielson (1978): $f_c^* = (0.7 - f_c'/200)f_c'$

Ramirez (1984): $f_c^* = 30\sqrt{f_c'}$ (f_c' units: psi.)

Schlaich (1982) observed that compression struts have their least width at the nodal points and in many cases can increase in width between the nodal points. This induces tensile stresses transverse to the strut which in turn limits the compressive strength of the strut. Schlaich therefore proposes an effectiveness factor related to the change in width of the strut over its length.

Collins and Mitchell (1984) and Vecchio and Collins (1982) have related the effective concrete strength to the principal tensile strain ϵ_1, at right angles to the direction of the principal compressive stress:

$$f_c^* = f_c'/(0.8 + 170\epsilon_1) \qquad (2.1)$$

The principal tensile strain ϵ_1, is obtained from Mohr's circle for strain as:

$$\epsilon_1 = \epsilon_x + (\epsilon_x + \epsilon_{2m})/\tan^2\theta \qquad (2.2)$$

where ϵ_x is the strain in the x direction, and ϵ_{2m} is the maximum compressive strain which Vecchio and Collins take as 0.002.

Rogowsky (1983) observed that the selection of an appropriate truss was more important than the selection of ν. A poor choice of a stress field may result in incomplete redistribution of forces and the premature failure of the truss, giving the appearance of a low value of ν.

Generally the strength of concrete in the nodal regions is taken as the value of f_c^* used in the struts. The 1984 Draft Canadian code however, recommended the following values for f_c^* :

1. 0.85 f_c' in nodal zones bounded by compression struts and bearing areas.
2. 0.75 f_c' in nodal zones anchoring only one tension tie.
3. 0.60 f_c' in nodal zones anchoring tension ties in more than one direction.

These values reflect the nonuniform stress fields due to the anchoring of tension ties in the nodal zones. This suggests

that in some cases a lower effective concrete strength might be used in the nodal zones than in the struts. The higher value of ν in the struts would generally be of little significance since the size of the nodal areas would control the design.

2.3 Advanced Stress Fields

The requirements outlined in the previous section are representative of this particular model only. Other, generally more complicated, models may make use of the tension capacity of the concrete, but of course this additional capacity is only valid the first time a member is loaded with a specific load case. Neglecting tensile forces carried by the concrete is therefore reasonable for a real situation which will have multiple load cases and therefore a varied crack pattern. In addition, different load conditions could lead to the use of more complicated stress fields such as decentred fans and biaxial nodal elements where σ_1 is not equal to σ_2 etc. These elements are discussed more fully by Thürlimann et. al. (1983).

3. EXPERIMENTAL PROGRAM

3.1 Test Specimens

3.1.1 Introduction

Five two span continuous beams were tested, all of which had a span to depth ratio, a/d, of approximately 0.79. Beam 1 contained light vertical web reinforcing steel, while Beam 2 had very heavy vertical web steel. Beams 3, 4 and 5 contained a medium amount of vertical web steel. None of the beams contained horizontal web reinforcement. All beams were symmetric about the centreline of the interior support column.

Beams 1, 3, 4 and 5 had identical external dimensions, while Beam 2 had a reduced depth, larger load columns and larger support columns. The beams were loaded and supported through column stubs cast integrally with the beam to provide a realistic load introduction and support system.

All of the beams, with the exception of beam 2, were loaded initially until one of the two interior shear spans failed, and then were retested to fail the other interior shear span. In the case of Beam 2, the beam was too severely damaged in the initial test to allow a retest. The retests were made possible by the use of an external reinforcing yoke placed on the shear span which failed in the initial test.

3.1.2 Selection of Variables in Test Program

Rogowsky's (1983) study of deep beams revealed that, in general, plastic truss models provide good predictions of ultimate capacities and truss member forces, provided that an appropriate stress field has been selected. He found that the stress field which predicted reactions close to those experienced in the real structure was the best choice. In other words, allowance must be made for the reaction force distribution due to creep, shrinkage, and support movements, etc.

Two specific observations pertinent to the present study were:

1. Beams with heavy stirrup reinforcement exhibited considerable ductility. In Rogowsky's tests these beams did not exhibit the characteristic reduction in shear strength, v_u/f'_c, with increasing a/d ratios. For the four a/d ratios tested by Rogowsky the v_u/f'_c ratios appeared to be consistently approximately 0.13 for the beams with heavy web reinforcement.
2. Continuous deep beams with very little web steel failed to redistribute forces within the truss members to allow the top chord to yield. Rogowsky suggests that the lack of ductility in these beams did not allow for complete redistribution. It has been noted that reinforcement details may have also contributed to premature failure or incomplete

redistribution within the beams.

These two observations have each led to the testing of one beam within the current study, Beams 1 and 2, respectively.

Rogowsky proportioned his top and bottom chord steel areas based on the elastic bending moment distribution in the uncracked elastic beam. Provided that sufficient ductility exists in the truss members, however, appropriate stress fields should be able to be drawn for a wide range of top and bottom chord steel areas. This premise led to the testing of Beams 3, 4 and 5 in the current study. In these beams the relative amounts of top and bottom chord steel were varied, while the total area of chord steel remained constant.

3.1.3 Details of Specimens

The overall dimensions and reinforcing steel layouts for the each of the five beams are shown in Figures 3.1 to 3.5. Details of the reinforcing steel in each specimen are presented in Table 3.1. In all cases the main longitudinal steel passed inside the vertical column bars. Clear cover to the column ties was 15 mm while cover to the stirrups at the sides of the beam was 35 mm for Beams 1, 3, 4 and 5 and 30 mm for Beam 2 which used larger 10M stirrups. Vertical clear cover to the stirrups and longitudinal steel at the top and bottom of the beams varied depending on the requirements dictated by the stress field used to design each beam. Dimensions to the centreline of each layer of steel in the

Table 3.1 Reinforcing Steel Details

Specimen	Top Steel			Bottom Steel			Vertical Web Steel (Int. Shear Span)		a (mm)	a/d**
	Bars	$A_s f_y$/bar (kN)	d (mm)	Bars	$A_s f_y$/bar (kN)	d (mm)	Bars	$A_s f_y$/stir* (kN)		
1	4-20M	132.0	946	3-20M	132.0	959	4-6M	28.8	750	0.79
2	4-20M	123.0	827	4-20M	123.0	827	11-10M	87.0	650	0.79
3	4-20M	123.0	946	3-20M	123.0	959	10-6M	28.8	750	0.79
4	3-20M	123.0	959	4-20M	123.0	946	10-6M	28.8	750	0.79
5	5-20M	123.0	951	2-20M	123.0	959	10-6M	28.8	750	0.79

* Value given is for a two leg stirrup. $A_s f_y$/bar is equal to $A_s f_y$/stir divided by two

** Based on average d for top and bottom steel

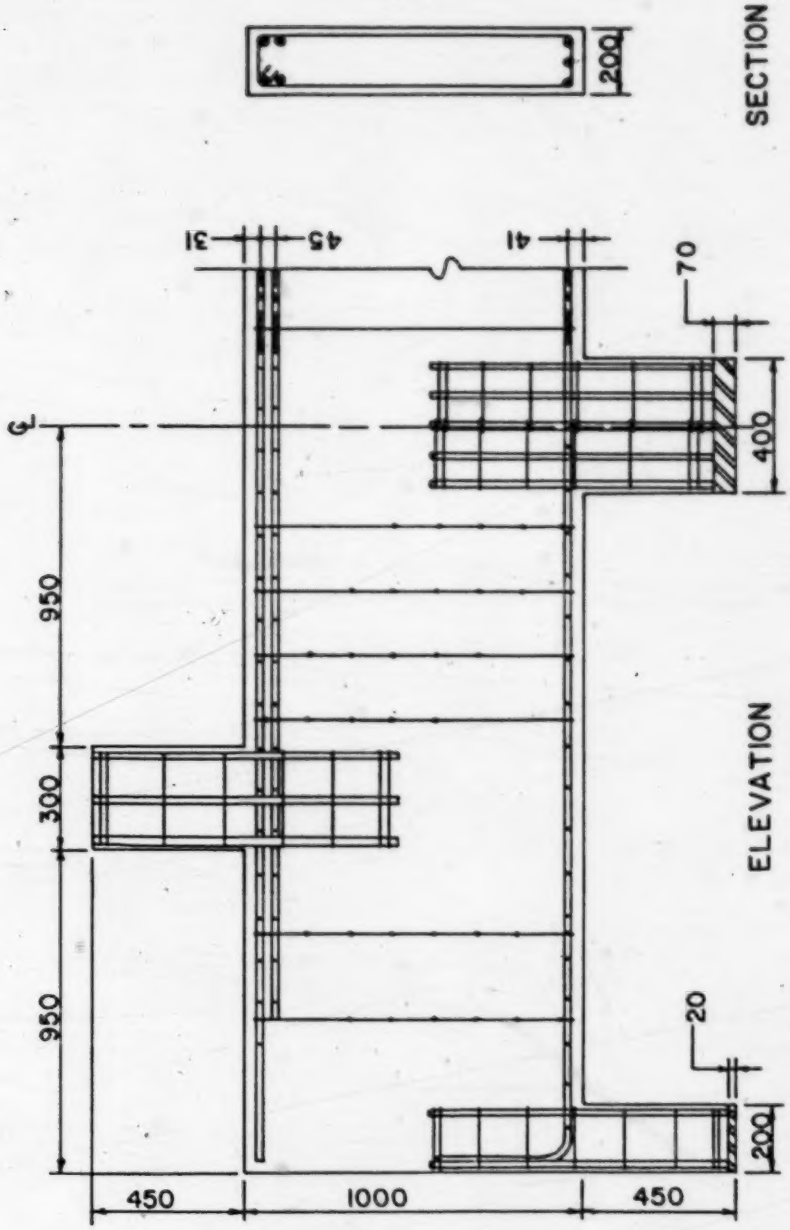

Figure 3.1 Beam I: Dimensions and Details

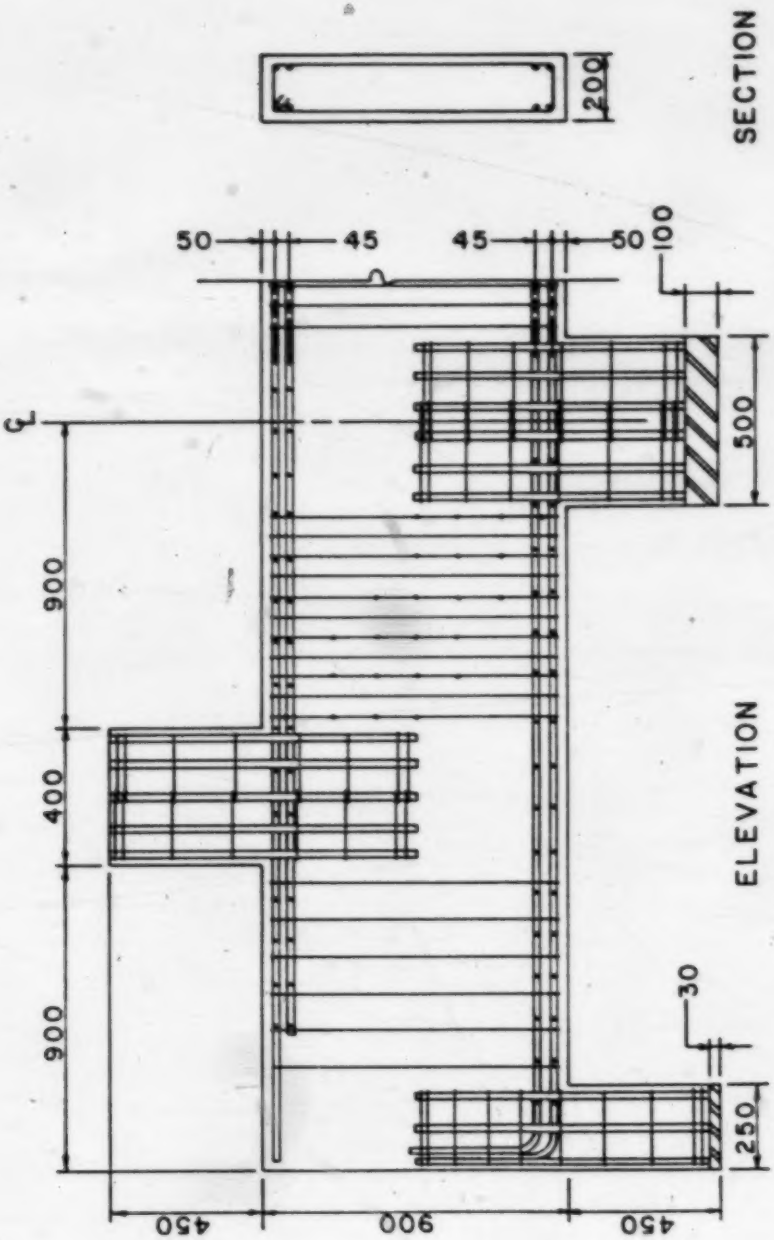

Figure 3.2 Beam 2: Dimensions and Details

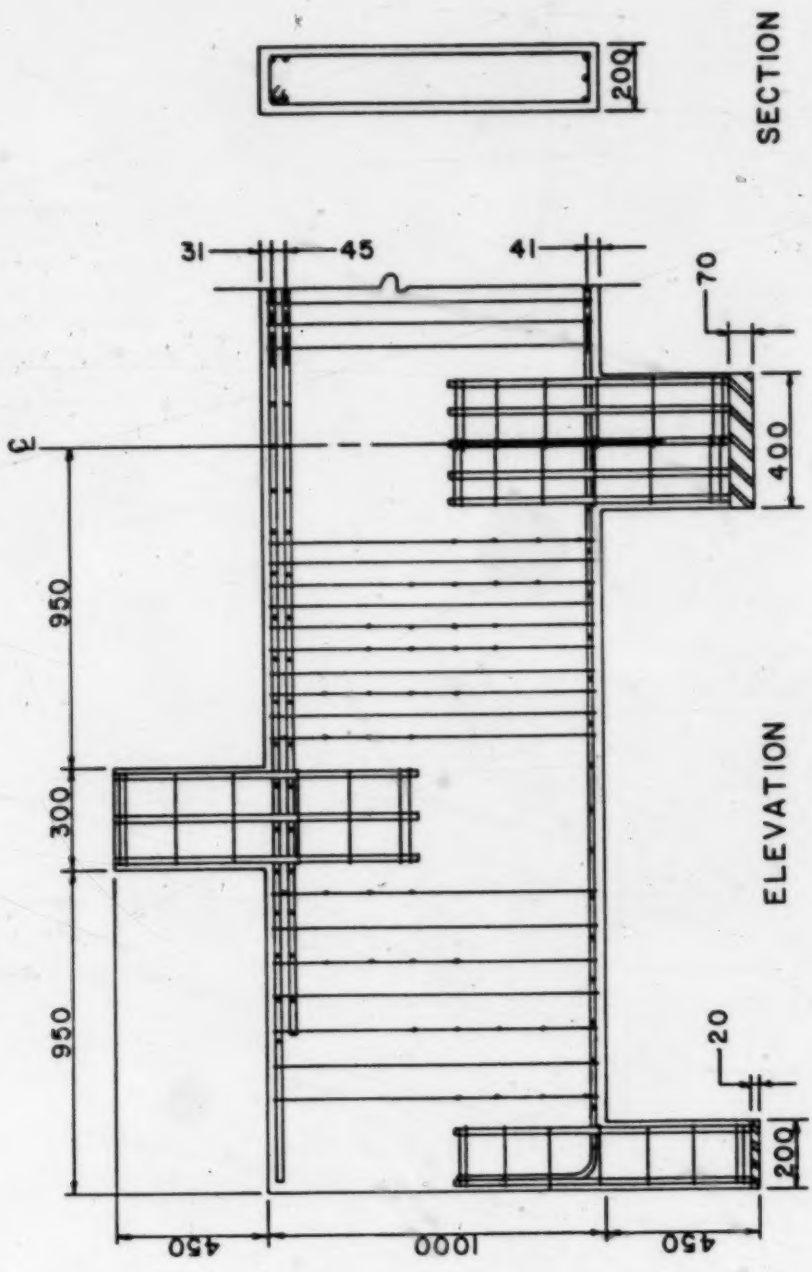

Figure 3.3 Beam 3' Dimensions and Details

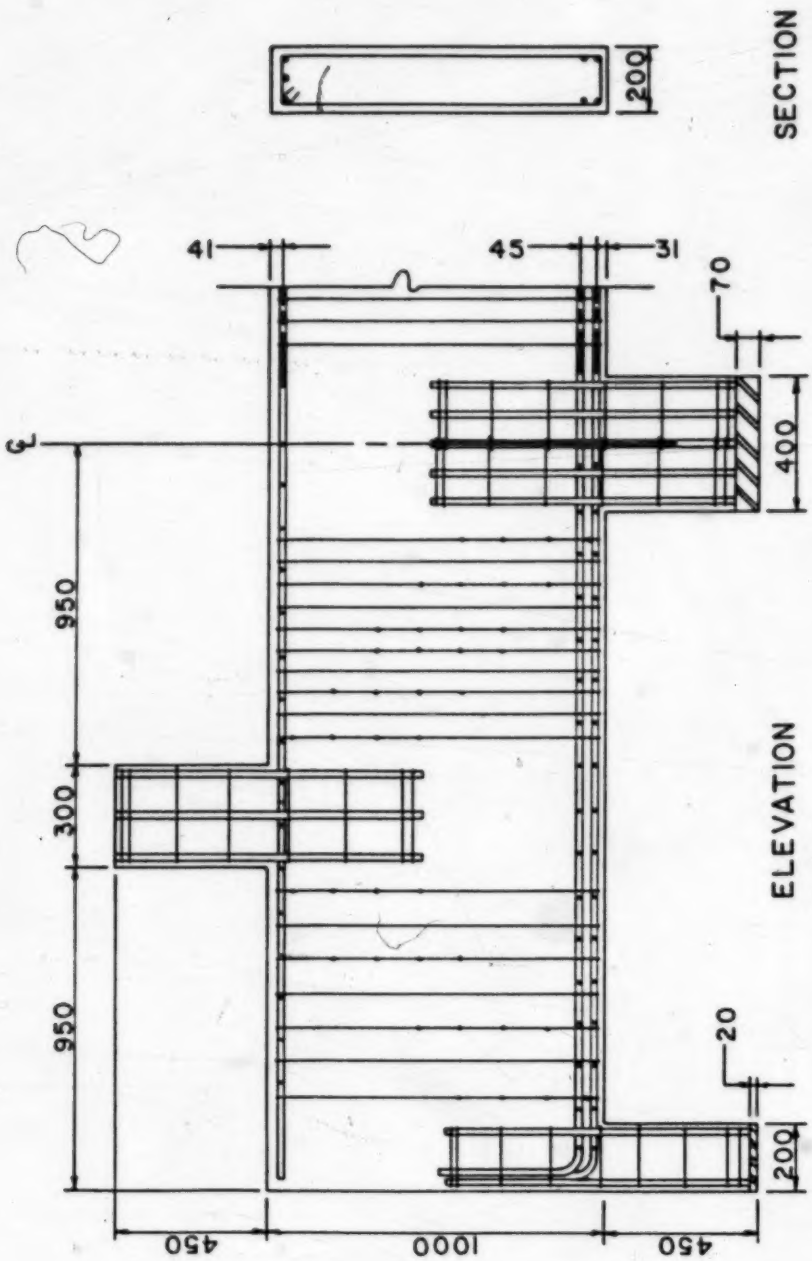

Figure 3.4 Beam 4: Dimensions and Details

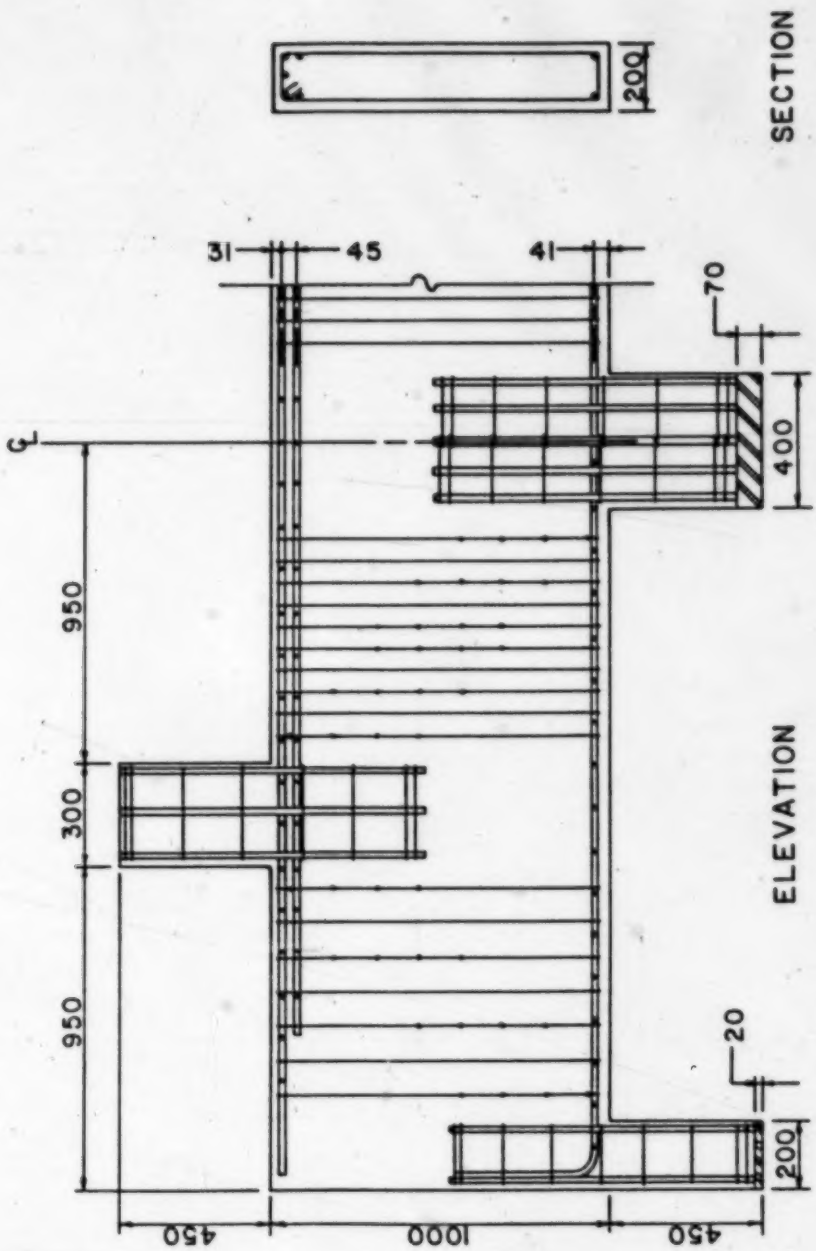

Figure 3.5 Beam 5: Dimensions and Details

beams are shown in the figures.

All of the bottom longitudinal steel extended the full length of the beams and was anchored by standard 90 degree hooks located within the exterior column cages. The upper layer of the top longitudinal steel extended the full length of the beams. In cases where a lower layer was present, the steel in this lower layer was carried at least one tension development length past the exterior face of the loading columns. All column steel extended at least one compression development length into the beam. The vertical stirrups were all closed and anchored at the top by 135 degree hooks around a longitudinal bar. The stirrups were arranged so that the hooks were always at the top of the beam but were placed with the hooks alternating from the east to the west side of the beam.

Lifting loops were provided near the end of each beam and above the centre support column. The loops consisted of 1/2 inch diameter prestressing strand.

3.2 Materials

3.2.1 Reinforcing Steel

3.2.1.1 Steel Properties

All reinforcing steel, with the exception of the column ties, consisted of deformed bars. The column ties were 6 mm diameter cold rolled smooth bars.

The testing to determine the stress-strain characteristics of the steel was conducted primarily in a MTS testing machine, and to a limited extent in a Baldwin testing machine. Strain readings were taken using two electrical strain gages mounted opposite each other on the reinforcing steel. The gages were arranged in a full bridge circuit so that the average strain was obtained. Some bars were also tested using a Demec gage (demountable mechanical extensometer) to eliminate the effect of reducing the area of the steel specimen for the application of strain gages. Generally this effect was found not to be significant, with the exception of the 6 mm steel in which a reduction in the yield load of up to 7% was apparent.

Brazing was employed as the method for fastening lugs to the reinforcing steel. Demec targets were subsequently fastened to the ends of the lugs with sealing wax. This method allowed the direct measurement of the elongation of the reinforcing steel using Demec gages. The effect of brazing on the properties of the reinforcing steel was investigated by testing specimens with and without brazing. It was found that the brazing did not significantly affect the yield strength or ultimate tensile strength, but did reduce the overall ductility of the 6 mm steel. This effect combined with the 'roundhouse' nature of the 6 mm stress-strain curve made it a less than ideal material in the plasticity sense. Brazing appeared to have no effect on the 10M and 20M bars.

The results of the material tests are presented in Table 3.2 and in Figures 3.6 and 3.7. The tabulated values for the yield strength, f_y, are based on the nominal areas for 10M and 20M bars, and on a calculated area for the 6 mm steel derived from weighing a 6 mm bar. Due to the roundhouse nature of some of the load-deformation curves, the yield strengths were obtained using the 0.2% offset method.

3.2.1.2 Assembly

The reinforcing steel cage was assembled to ensure that the longitudinal steel was generally within 2 to 3 mm of its specified position. The stirrups were more difficult to place but were always within 15 mm of their design position measured parallel to the beam span. Approximately one half of the bars in a column were tack welded to the base plates to allow for easier fabrication of the cage. The cage itself was tied together using 18 gage tie wire.

Steel lugs were brazed to the reinforcing steel at locations where Demec gage readings were to be taken, as well as at a few other locations to ensure the proper positioning of the cage in the formwork. In some instances plastic chairs were also employed to hold the cage in place during the concrete pour.

To prevent any lateral force acting on the steel lugs due to bond slip between the concrete and the reinforcing steel, a gap was left around each lug. This was accomplished by rubbing vaseline on the lugs and placing a piece of

Table 3.2 Reinforcing Steel Properties

Bar Size (mm)	Heat	$A_s f_y$ (kN)	Yield Strain ($\mu\epsilon$)	A_s (mm^2)	E_s (MPa)	f_y (MPa)
20	1	123.0	1900	300	219000	410
20	2	132.0	2300	300	206000	440
10	1	43.5	2050	100	203000	435
6	1	14.4	2200	31.9	190000	451

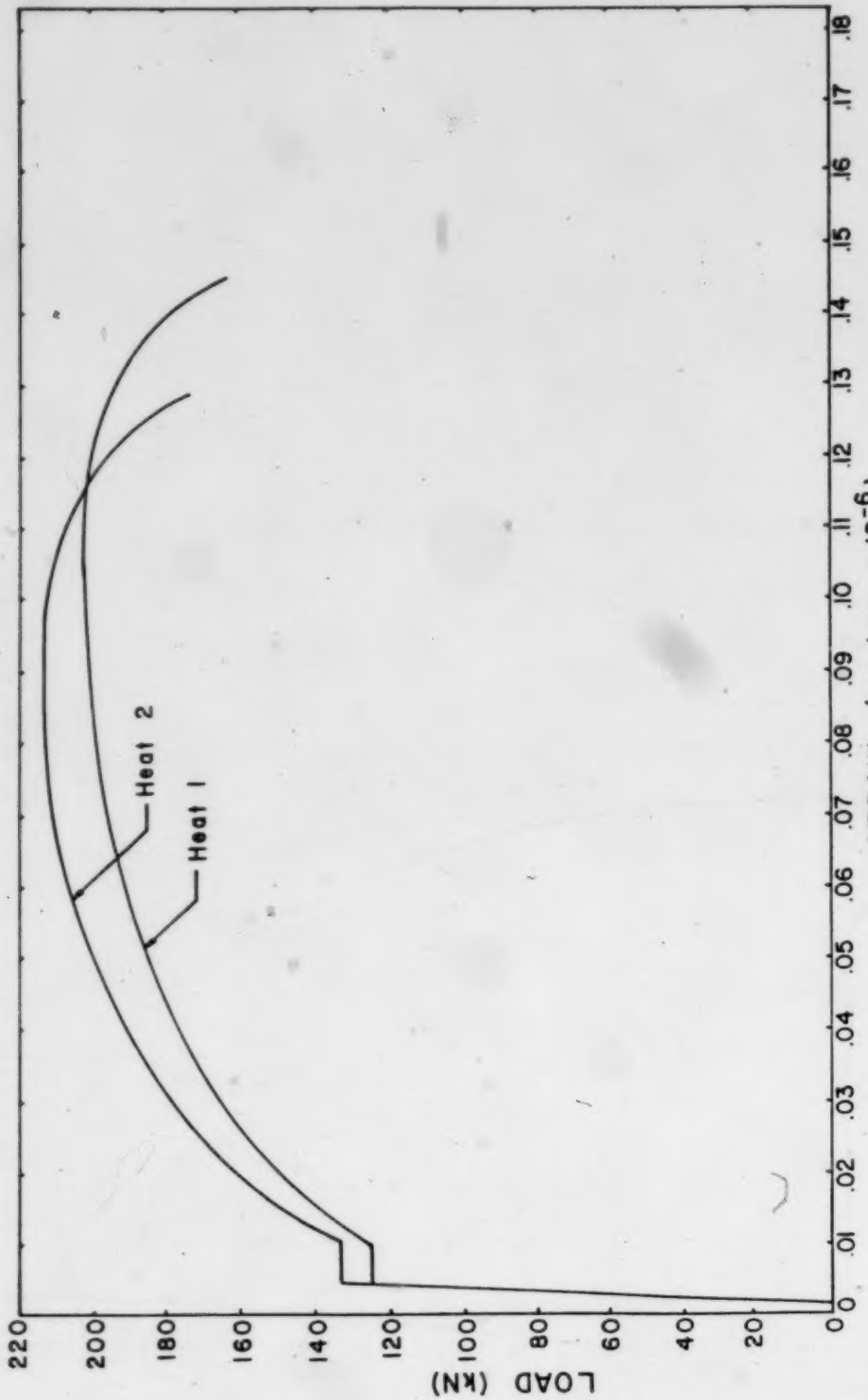

Figure 3.6 20M Steel Load-Deformation Curves

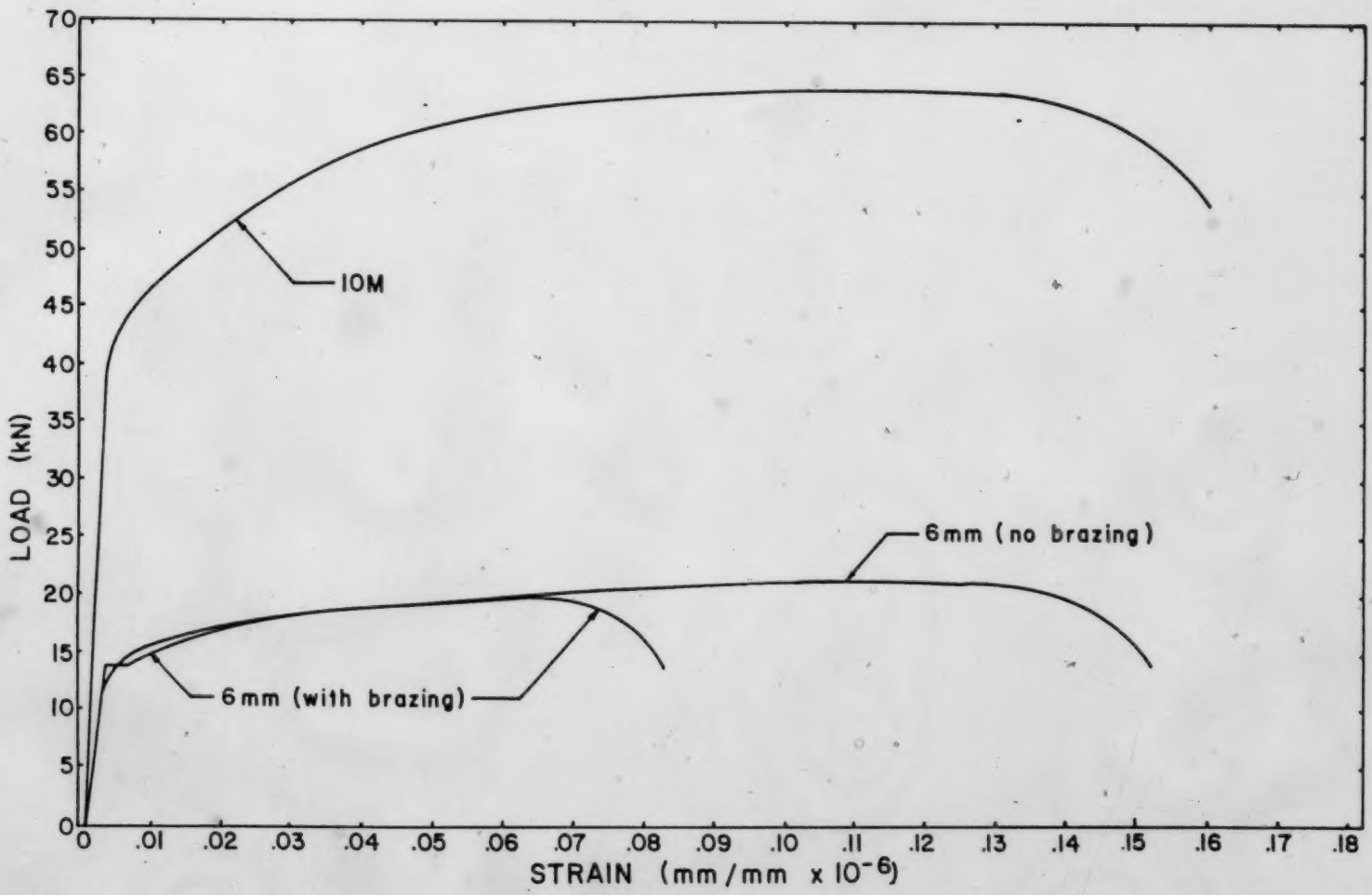

Figure 3.7 10M and 6 mm Steel: Load-Deformation Curves

rubber hose around them extending from the reinforcing steel to the sides of the forms. The hose was then covered with vaseline and a small strip of polyethylene was subsequently wrapped around the hose. Following the concrete pour the rubber hose was removed, leaving approximately 3 mm clear space around the lug.

3.2.2 Concrete

All of the concrete used in the tests was batched by a local concrete supplier. The design strength requirement was 30 MPa at 28 days. The mix design is shown in Table 3.3. A superplasticizer was employed to allow a higher slump mix. This ensured ease in placement while at the same time maintained a reasonable water-cement ratio. This resulted in slumps in the range of 5 to 9 inches at the time of placement as well as adequate cylinder test strengths.

The concrete for one beam was placed in approximately one hour following the arrival of the truck. Placement was aided by the use of common immersion type pencil vibrators.

The formwork was removed approximately 24 hours after placement. The beams were then cured with wet burlap and polyethylene sheets for 4 days. After this curing period the beams were stored in the lab with no special curing procedures. Nine cylinders were cast at the same time as the beams, and were then cured in a similar manner to the beams.

Two of the nine cylinders were tested at 7 days in a standard compression test in accordance with CSA Standard

Table 3.3 Concrete Mix Design

ITEM	MASS (kg/m^3)
Cement - Type 10	270
Fly Ash	70
Sand	757
Rock - 14 mm	1060
Water	135

Note: Superplasticizer and Air Entraining Agent also used.

A23.2. These cylinders gave an indication of the rate of strength gain, and were used to obtain a general assessment of the quality of the concrete.

The remaining 7 cylinders were tested on the same day as the initial beam test or on the following day. One was used for a split cylinder test (CSA A23.2-13C) while the remaining six were tested in compression. Three of these cylinders were used to determine the modulus of elasticity, E_c. The results of the compression tests, and the modulus of elasticity tests were very consistent for each beam, indicating uniformity of material in the cylinders. Plots of the stress-strain data indicated a linear response up to at least 50% of f_c'. The concrete properties are summarized in Table 3.4.

3.3 Instrumentation

3.3.1 General

The specimens were instrumented in a variety of ways. All loads and reactions were measured with load cells. The steel and concrete strains were measured using Demec Gages, while displacements were measured with dial gages and Linear Variable Displacements Transformers (LVDT's). Loads, reactions and midspan deflections were recorded automatically using a computerized data aquisition system. The strains and the deflections of the ends of the specimens were recorded by hand.

Table 3.4 Concrete Properties

BEAM	f'_c (MPa)	f_t (MPa)	E_c (MPa)	AGE (days)
1	35.4	—	25600	52
2	31.3	2.7	21700	42
3	27.8	—	21000	56
4	35.9	3.0	25300	50
5	31.1	3.0	23900	48

In addition to this instrumentation at each load interval, the crack development in the beam was monitored and marked on the beam with a black felt marker.

3.3.2 Loads and Reactions

The loads and exterior reactions were measured using Durham Instruments FTC-A100 400k load cells with a range of 0 to 1780 kN and an accuracy of ± .1 kN. The interior reaction was measured using a Durham Instruments FTC-A100 600k load cell with a range of 0 to 2670 kN and an accuracy of ± .15 kN. The calibration of the load cells in the MTS testing machine in the lab indicated a very linear response. An overall check of statics indicated that throughout the tests the sum of the loads were generally within 2 kN of the sum of the reactions. The reactions, loads and shears reported in Chapters 4 and 5 are based on corrected reactions and loads in which the errors were balanced, as in a survey traverse.

3.3.3 Strains

The strains were measured using a Demec gage which measures the change in distance between targets attached to the specimens. The steel strains were measured on the west face of each specimen, while the concrete strains were measured on the east face.

In the case of the steel strain measurements, a 5 inch (127 mm) gage length was employed. The targets were attached

with sealing wax to 6.3 mm diameter steel lugs which were in turn brazed to the reinforcing steel as described in section 3.2.1.2. Gage locations are shown in Figures 3.1 to 3.5 as dots on the reinforcing bars. The readings were made visually from a dial on the Demec gage, and recorded by hand. The least count on the dial represented 9.8 microstrain. The repeatability of the readings was very much dependant on the consistency of the instrument man in applying pressure. This was made more difficult by the flexing of the lugs attached to the reinforcing steel. However, it was found that consistent readings could be achieved with practice.

The concrete strains were measured using an 8 inch (203 mm) square grid as shown in Figure 3.8. This layout was chosen with the hope that a direct comparison could be made between the results of these tests and those of Vecchio and Collins (1982). In this test series the targets were mounted directly on the concrete with sealing wax. Readings were taken with a Demec gage along an 8 inch (203 mm) gage length on the horizontal and vertical sides of each square, as well as along the 11.3 inch (287 mm) diagonals. In the case of the 8 inch gage, the least count on the dial represented 9.7 microstrain while on the 11.3 inch gage this represented 7.0 microstrain. Repeatability was very good with both gages. There is redundancy in the number of strain readings for each square. Only three are needed to obtain principal strains, while six were taken. From each square it was then

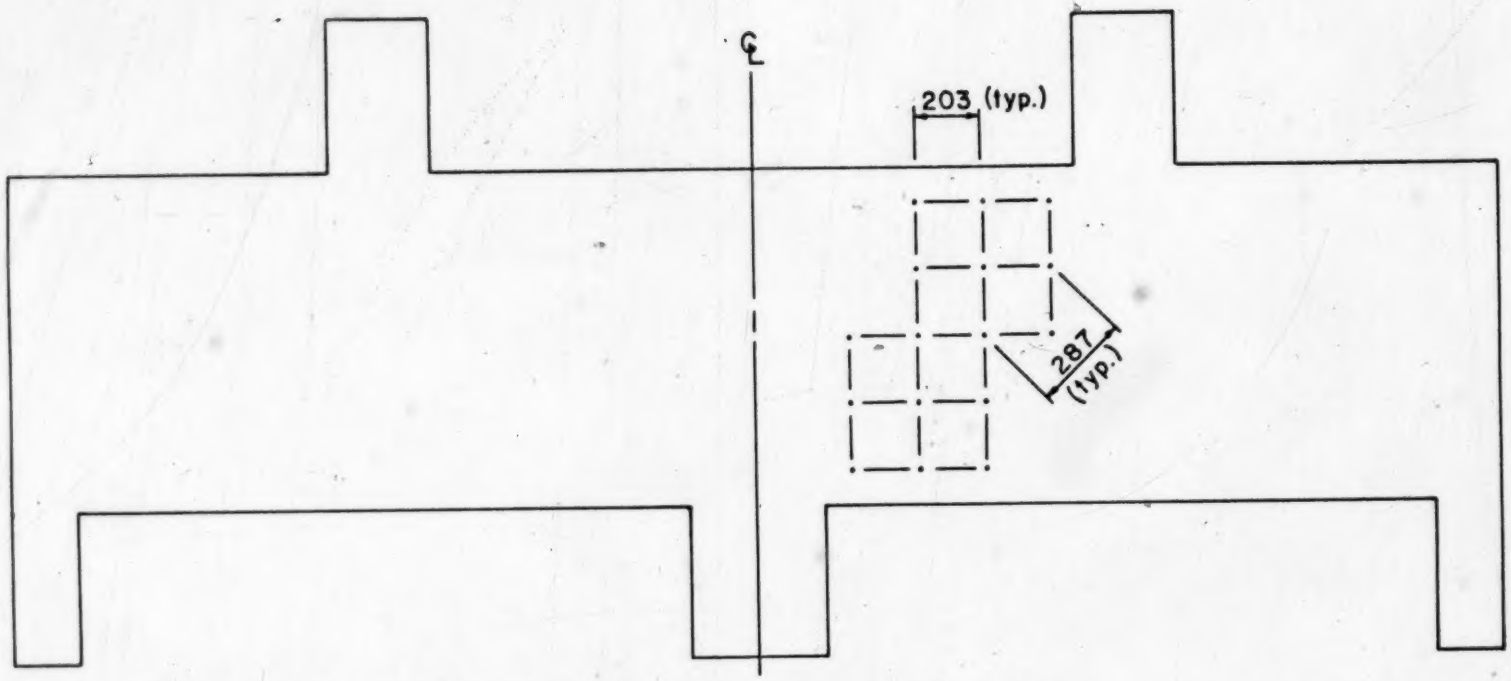

Note: Pattern is shown as seen on the east face of the specimen.

Figure 3.8 Concrete Demec Target Layout

possible to draw 12 Mohr's Circles of strain yielding 12 sets of principal strains. It was intended that these could be determined and averaged to give a good estimate of the state of strain in each square element. As discussed in Chapter 5 there was a wide disparity within each set of 12 circles.

3.3.4 Displacements

The midspan deflections of each span and the settlement of the central support were measured with Hewlett Packard model 7DCDT-500 LVDT's which had a full scale output of 6 volts DC with a full scale displacement range of ± 12.5 mm. Calibration curves indicated a very linear response throughout this range.

The horizontal displacements of the north and south ends of the beams were measured at midheight of the beam with dial gages which had a least count of 0.01 mm. These measurements were taken in order to determine if the beam had undergone any overall movement in the north-south direction which could cause a stability problem. Hydraulic rams were located at each end of the specimen to bring the specimen back into position in the event that movement occurred. These rams were never required during the course of the test program.

3.4 Testing

3.4.1 Test Set-Up

The test specimens were tested in the loading frame shown in Figure 3.9. The specimen was loaded using 1780 kN capacity hydraulic rams which were pressurized with an 'air on oil' system. This system maintained a constant load, providing that the rams did not travel too quickly or reverse their direction of travel. This resulted in the test being load controlled at least until the peak load was attained. This load system ensured that the applied load was maintained during the periods when the strain measurements were recorded.

3.4.2 Test Procedure

The loads were applied in increments of approximately 50 kN, each application taking approximately 5 minutes. After each increment of load, the load was maintained as a set of load, reaction and displacement readings were recorded through the data aquisition system. The cracks were also marked on the beam with a black felt pen. These readings took an average of 10 minutes to complete. After several load increments were applied, the steel and concrete strain readings were recorded. Partial sets of strain readings were taken with greater frequency towards the end of the tests in critical areas of the beam. A complete set of strain readings took on the average, 45 minutes. Five to

Figure 3.9 Test Frame and Set-Up

7 sets of strain readings were taken during each test. The testing procedure required from 6 to 8 hours to complete through to the failure of the first shear span.

On the day following the initial test for each beam, external stirrups consisting of steel yokes and 12-3/4" diameter vertical tie rods were used to reinforce the failed span, and the beam was then retested until the other interior shear span failed. Plaster was placed on the top surface of the beam to compensate for any irregularities. The tie rods were tightened as much as possible with an air powered wrench. This procedure often caused many of the cracks of the previously failed span to close up.

Retesting of the specimen proceeded in much the same manner as the initial test. As the main purpose of the retest was to confirm the failure mode, a reduced number of strain measurements were taken. During the initial stages of the retest, the distribution of the reaction loads was not as would be expected. Due to the permanent deformations present in the specimen as a result of the initial test, the reactions did not stabilize until the loads reached approximately 50 kN.

4. TEST RESULTS

4.1 Presentation of Results

This chapter presents the test results for all five specimens. An interpretation of these results is given in Chapter 5. Most of the results have been reduced to graphical form to facilitate interpretation. The measured failure loads and reactions are given, followed by the load deflection data. Finally, the individual beam results are presented. This section includes a description of observations made during the test, figures displaying the crack patterns, the principal compressive concrete strains and the steel strain data. In Figures 4.2, 4.5, 4.8, 4.11 and 4.14, the cracks are shown as solid black lines. Areas where the concrete appeared to have spalled or crushed are shown with light shading. All of the figures are drawn with the north end of the beam shown at the left side of the page, regardless of whether the data was obtained from the east or west face of the beam. The concrete strain data is therefore depicted as though viewed through the beam from the west.

4.2 Failure Loads

The measured loads and reactions at failure are given in Table 4.1. Also shown are the values of the shear V_u in the interior shear spans at failure, the shear stress computed from $v_u = V_u / bd$, and the ratio of shear stress to the

Table 4.1 Failure Loads, Reactions and Shear Strengths

Beam		North Support Reaction (kN)	North Jack Load (kN)	Interior Support Reaction (kN)	South Jack Load (kN)	South Support Reaction (kN)	V_u (kN)	v_u** (MPa)	f_c' (MPa)	v_u/f_c'
1	Initial	454	1204	1506	1200*	446	754	3.96	35.4	.112
	Retest	447	1295*	1707	1294	437	848	4.45	35.4	.126
2	Initial	532	1480*	1902	1481	529	948	5.73	31.3	.183
	Retest	—	—	—	—	—	—	—	—	—
3	Initial	419	1235	1652	1250*	414	836	4.39	27.8	.158
	Retest	439	1310*	1754	1304	420	871	4.57	27.8	.164
4	Initial	576	1502*	1866	1502	565	926	4.86	35.9	.135
	Retest	578	1552	1959	1568*	584	984	5.16	35.9	.144
5	Initial	307	1078	1544	1080*	306	774	4.05	31.1	.130
	Retest	336	1296*	1927	1299	329	960	5.03	31.1	.162

* Indicates failure span
** Based on average d

concrete compressive stress, v_u/f'_c. Both the initial and retest values are presented. An asterisk indicates the interior shear span which failed in each case.

Some of the reactions have been extrapolated from the last recorded load set as it was not always possible to record these values at the instant the beam failed. In these cases, the failure load was known since this value was monitored continuously during the test. The reactions were extrapolated to satisfy vertical equilibrium with the known loads. The distribution of the extrapolated reactions was in accordance with the proportions of the last recorded load set. This extrapolation of the reactions to balance the failure load never exceeded 30 kN in either span.

4.3 Deflections

The observed midspan deflections are presented in Figure 4.1 for both the initial tests and retests. The deflections are plotted for the span in which the failure occurred. Although some of the midspan deflection is due to support settlement, this contribution is not significant and is therefore not subtracted from the curves.

Only one curve is shown for Beam 2 since it was not retested. In the case of Beam 4, the deflection gage malfunctioned and therefore the retest curve is not given in the figure.

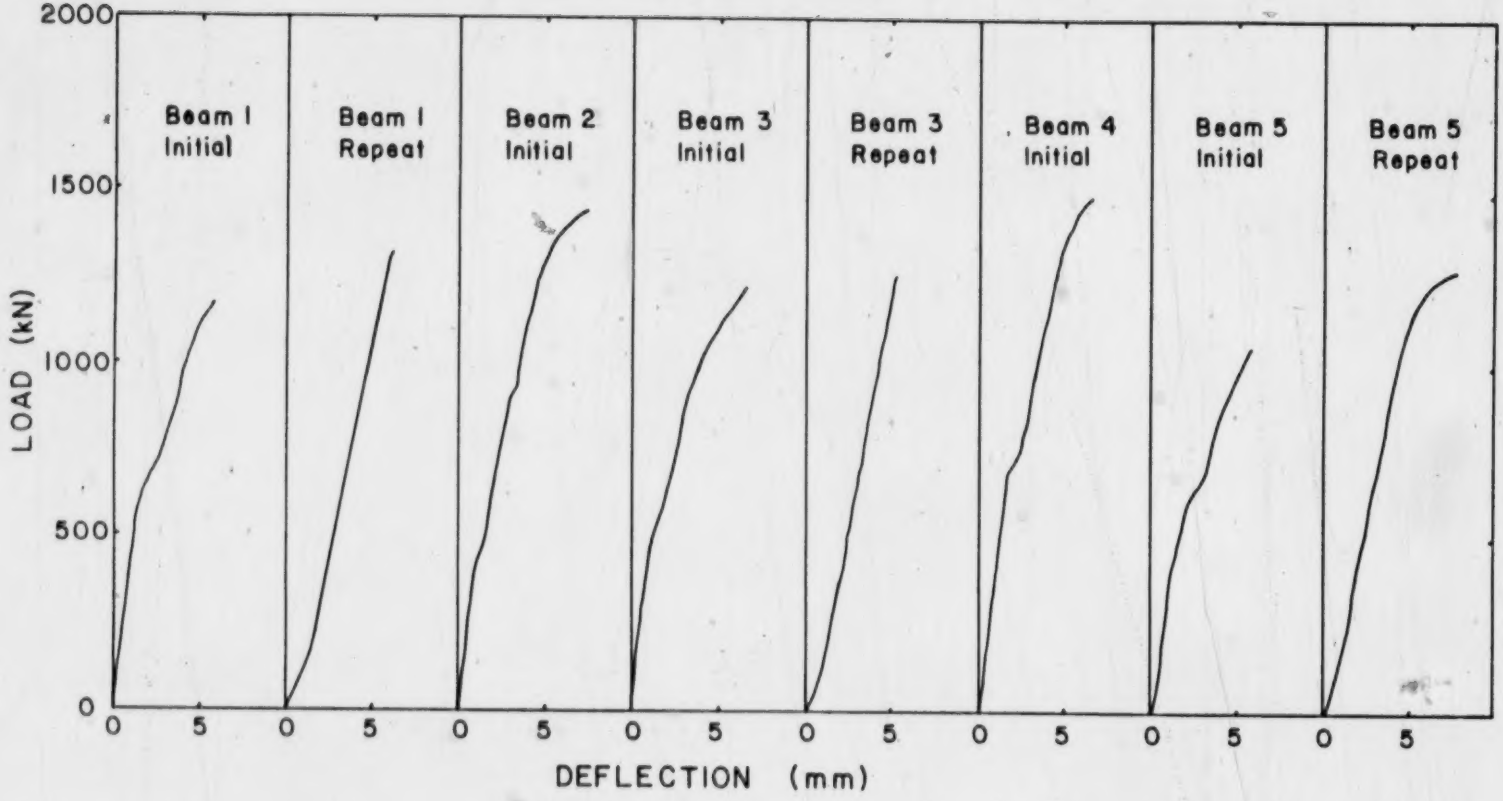

Figure 4.1 Load-Deflection Curves

4.4 Results of Individual Beam Tests

4.4.1 Beam 1

Flexural cracking initially occurred in both the positive and negative moment regions at a load of approximately 500 kN. Inclined cracks began to be observed at about 600 kN. Also at this load, a large diagonal crack appeared with a bang in the south interior shear span. These cracks ran from 4 inches below the top of the beam at the load column, to the interior support column where the column meets the beam soffit. A similar crack formed in the north span at a load of approximately 800 kN. The failure of the south span was initiated by the crushing of the concrete near the top of the beam at the south load column where the theoretical direct strut in the plastic truss model met the hydrostatic zone under the load column. This failure occurred at a load of 1200 kN with little warning. At this load the bottom chord had yielded at midspan while the top chord was only at about 62% of its yield strain. The bottom chord yielded at a jack load of 1100 kN.

During the retest there was very little new crack development until the load reached 1100 kN. At this load another large diagonal crack formed in the north interior shear span. The north span failed at a load of 1295 kN. Failure occurred suddenly with a loud popping sound. There was evidence of concrete spalling and crushing near the load column, the interior support column and at about midheight

in the theoretical direct strut. The crack pattern at failure is depicted in Figure 4.2.

In both the initial test and the retest, several stirrups reached their ultimate tensile strength and broke as the beam failed. The stirrup failures always occurred immediately above or below locations where the Demec gage lugs had been brazed to the stirrups. The measured strains in the stirrups indicated that all of them had yielded before a load of 1100 kN had been reached.

Principal compressive concrete strain data is plotted in Figure 4.3, for a jack load of 1100 kN (85% of the ultimate load in that span). These values of principal compressive strains and their corresponding directions were obtained by reducing only three of the six strain measurements obtained for each square element. The three measurements chosen were three compressive strains or in the rare case where only two compressive strains were available, the smallest tensile strain was also used. These clearly show the existance of a diagonal compressive strut from load to reaction. The largest measured compressive strain was 0.00110. A similar reduction of concrete strain data was used for all five beams. A general discussion of the concrete strain data is included in Chapter 5.

The steel strains are plotted in Figure 4.4 for a jack load of 1100 kN (92% of the ultimate load of the initial failure span).

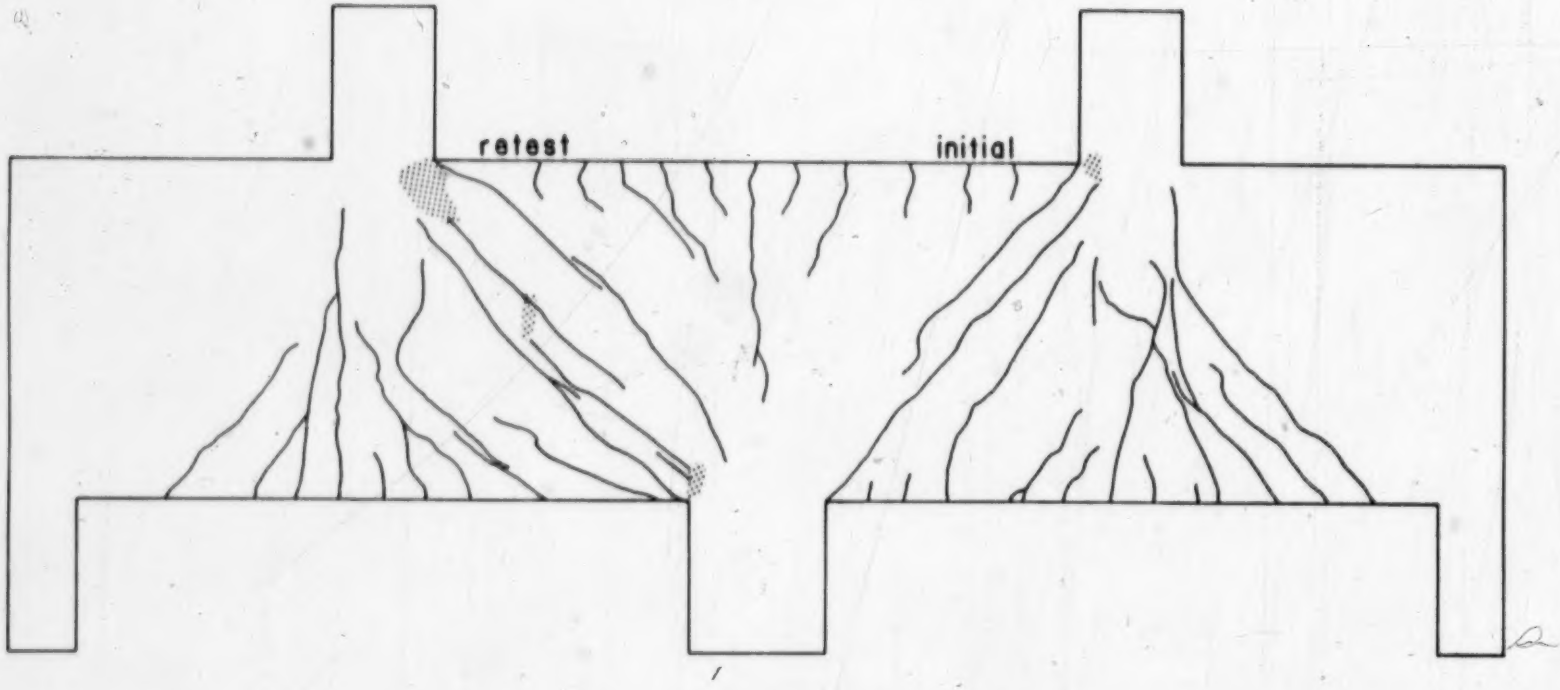

Figure 4.2 Beam 1: Crack Pattern

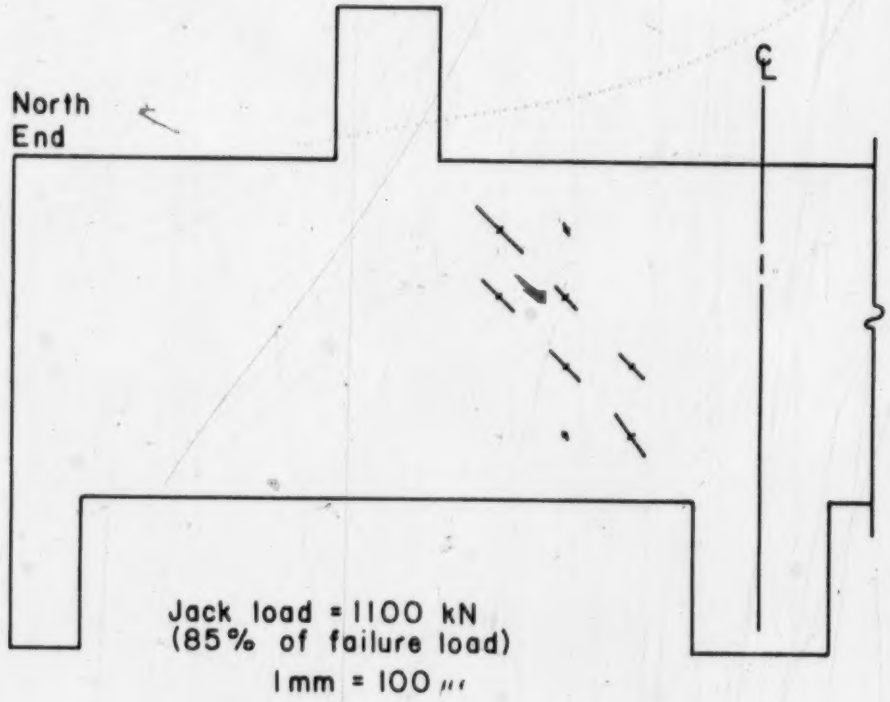

Figure 4.3 Beam 1: Concrete Compressive Strains

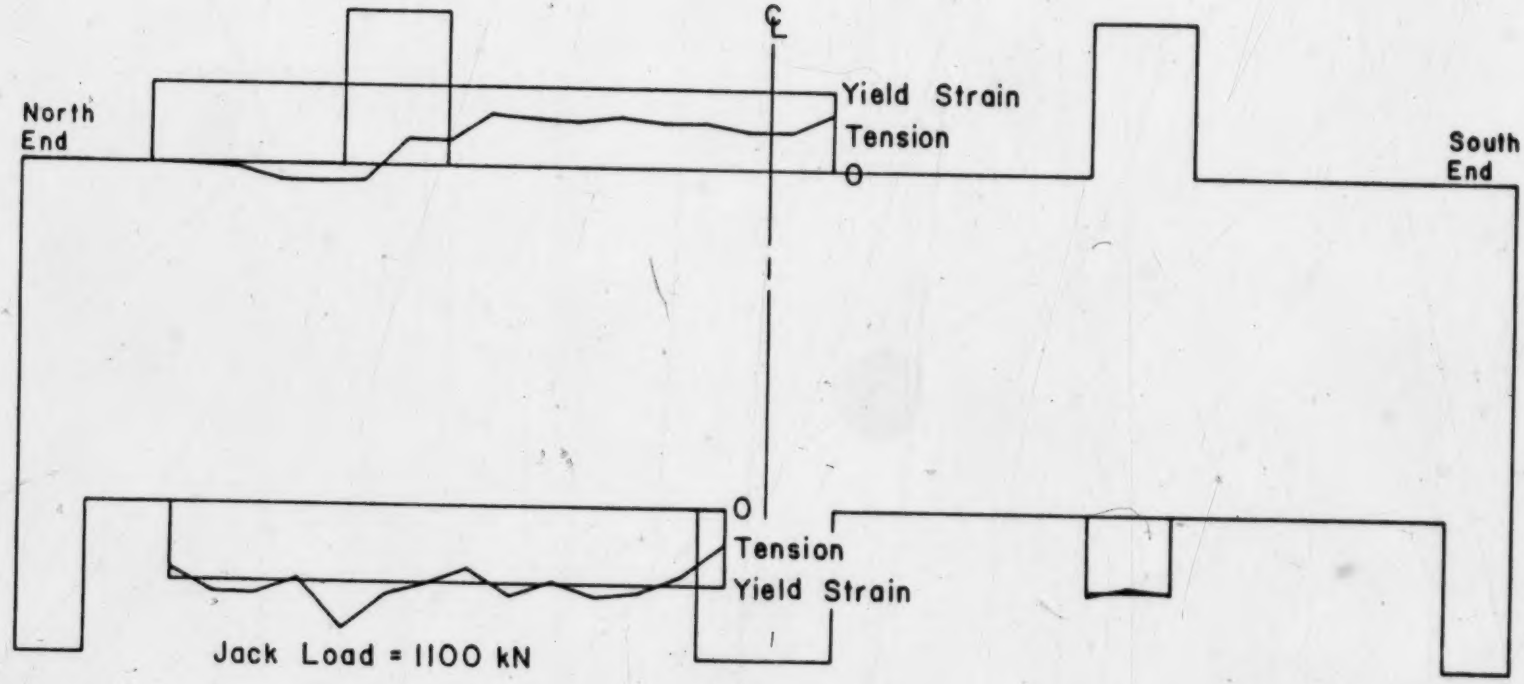

Figure 4.4 Beam I: Steel Strains

4.4.2 Beam 2

Flexural cracking initially occurred in both the positive and negative moment regions at a load of approximately 400 kN. At a load of about 600 kN, large diagonal cracks appeared in both interior shear spans. These cracks extended almost the full distance from the load column to the support column and formed with a distinctive popping sound. Failure occurred in the north interior shear span at a load of 1480 kN. It appeared to originate with some spalling near the load column, quickly moved vertically downwards through 1/2 of the depth of the beam, and then cracked diagonally towards the interior support column. The concrete was severely damaged through the entire depth of the beam. The failure was loud and explosive with small pieces of concrete landing up to ten feet away from the specimen. As a result of the extensive damage to the beam during the initial test, it was decided not to retest this specimen. The crack pattern at failure is shown in Figure 4.5.

At failure the longitudinal reinforcing steel had reached yield in both the bottom and top chords. The bottom chord yielded at a load of about 1200 kN (81% of the failure load) while the top chord did not reach yield until approximately 1400 kN (95% of failure load). All of the stirrups appear to have yielded at failure with the exceptions of the stirrup closest to the load column and the stirrup next to the interior support.

The principal compressive strains in the concrete are plotted in Figure 4.6 for a jack load of 1200 kN (81% of the failure load). The largest such strain was 0.00138. Steel strains at this load level are plotted in Figure 4.7. The large reduction in longitudinal steel strains towards the supports is consistent with the plastic truss model prediction for beams with a large amount of vertical web steel.

4.4.3 Beam 3

Flexural cracking first appeared in the positive moment region at a load of about 300 kN. In the negative moment region flexural cracks were not observed until a load of about 450 kN was attained. Following the formation of smaller diagonal cracks, a large diagonal crack running from the load column to the interior support column appeared in the south span at a load of approximately 1050 kN. Failure of the south interior shear span occurred at a load of 1250 kN. The failure originated with spalling and crushing of the concrete in the direct compression strut close to the load column. During the retest a large diagonal crack formed in the north span in a similar manner to the crack formation in the south span, at a load of approximately 1300 kN. Failure occurred at a load of 1310 kN and also appeared to be very similar in nature to the failure of the south span. The crack pattern at failure is shown in Figure 4.8.

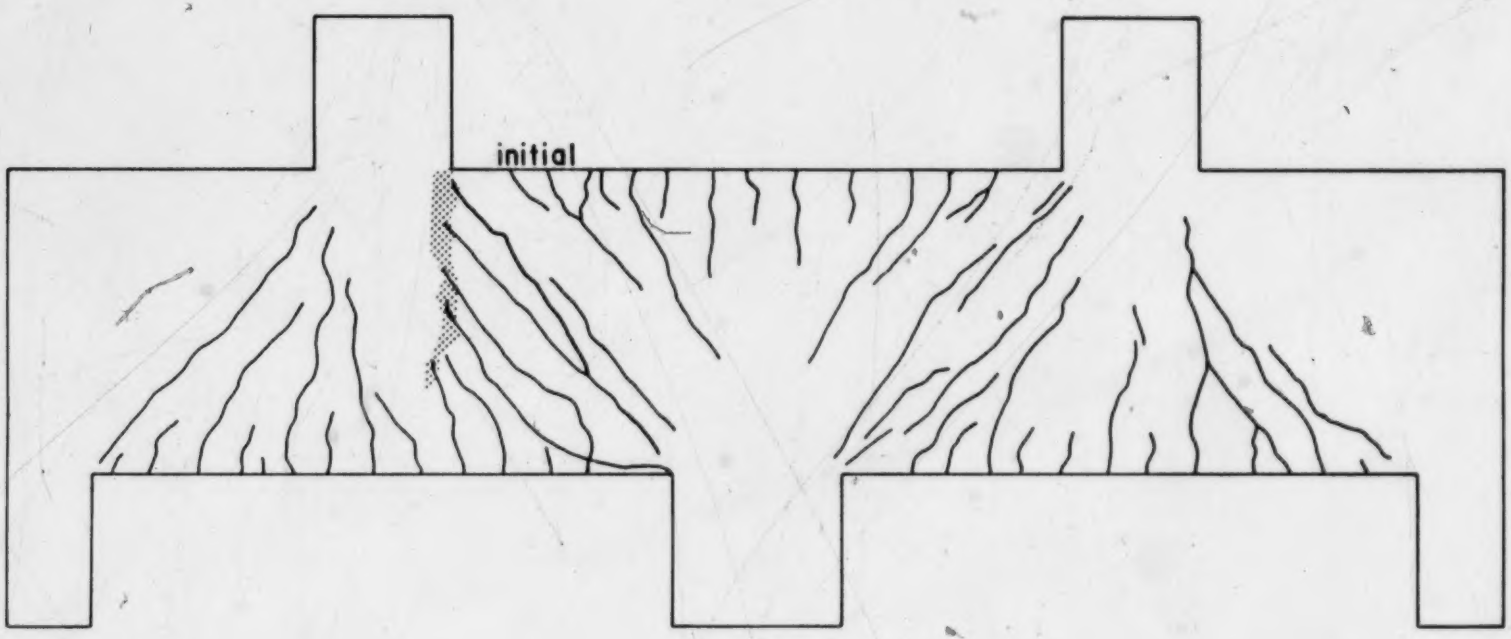

Figure 4.5 Beam 2: Crack Pattern

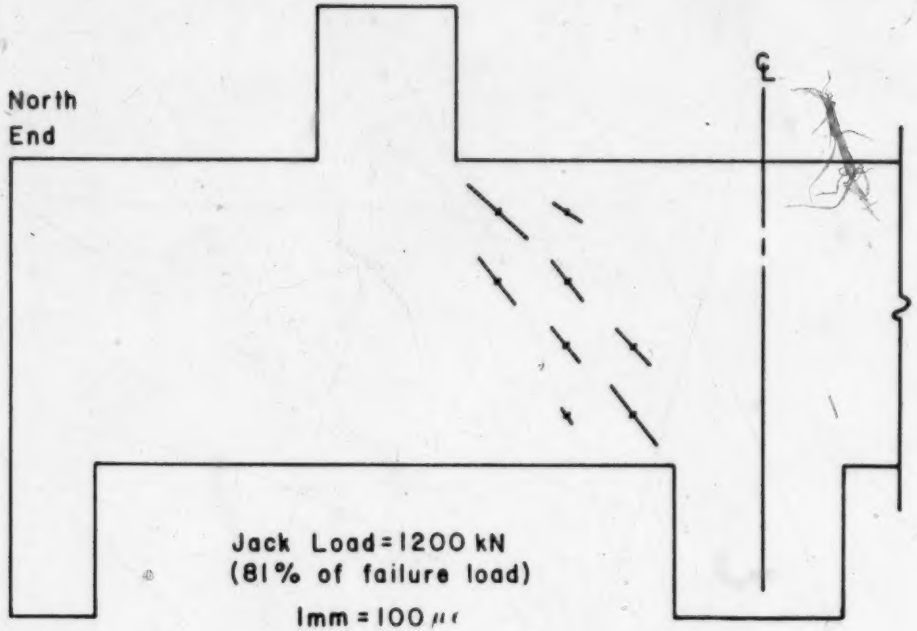

Figure 4.6 Beam 2: Concrete Compressive Strains

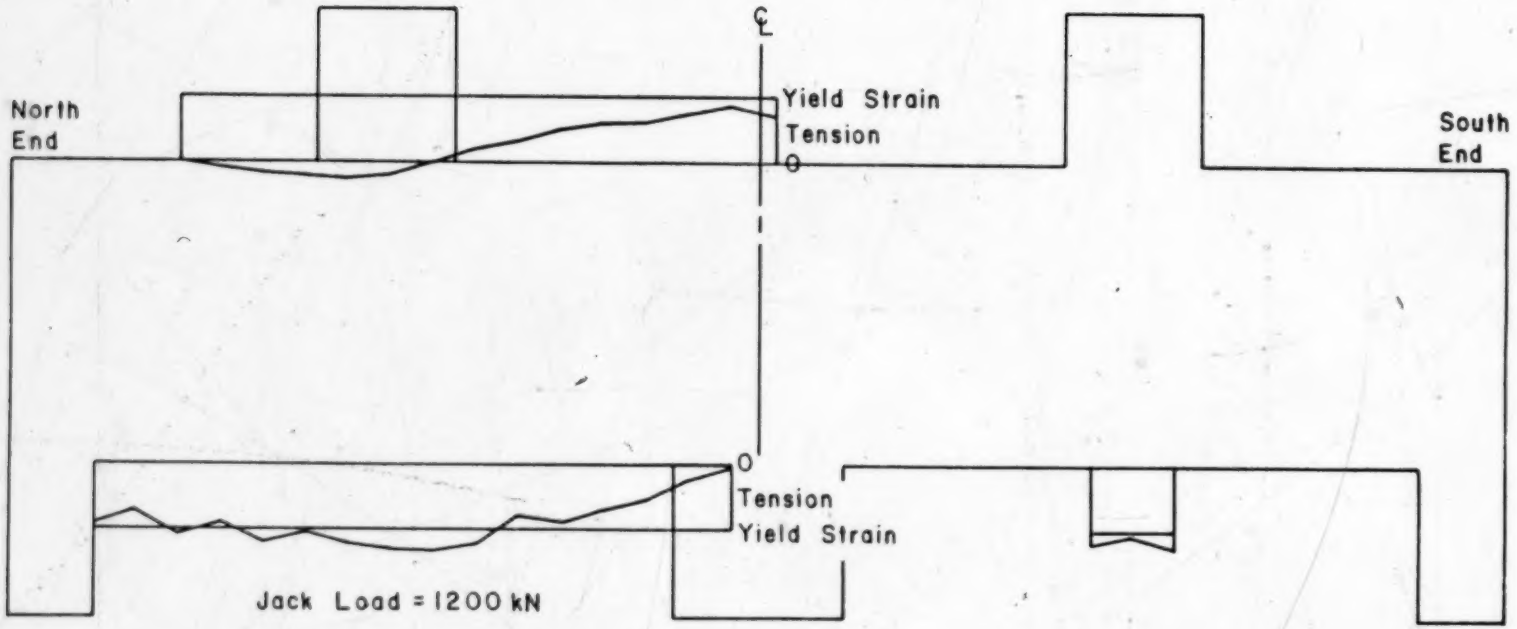

Figure 4.7 Beam 2: Steel Strains

The longitudinal reinforcing steel had reached yield in both the bottom and top chords at failure. The bottom chord yielded first at a load of about 950 kN (76% of the failure load). The top chord did not yield until a load of 1100 kN was reached (88% of failure load). All of the stirrups in the interior shear span had reached yield at failure, however the exterior shear span stirrups did not appear to have yielded. The principal compressive concrete strains are plotted in Figure 4.9 for a jack load of 1100 kN (88% of failure load). The largest such strain was 0.00108. Steel strains are also plotted for this load level in Figure 4.10.

4.4.4 Beam 4

Flexural cracking was initially observed in the positive moment region at a load of approximately 500 kN. In the negative moment region flexural cracks did not originate until a load of approximately 600 kN was reached. Following the formation of small diagonal cracks, a large diagonal crack appeared with a bang in the north interior shear span at a load of about 700 kN. A similar crack appeared in the south interior span at a load of about 725 kN. Failure of the north interior span occurred while holding at a load of 1500 kn. It initiated with some crushing of the direct compression strut near the load column, followed by a sudden fracture of the stirrups about 20 to 30 seconds later. Consistent with Beam 1, these stirrups failed at the locations where the lugs had been brazed to the reinforcing

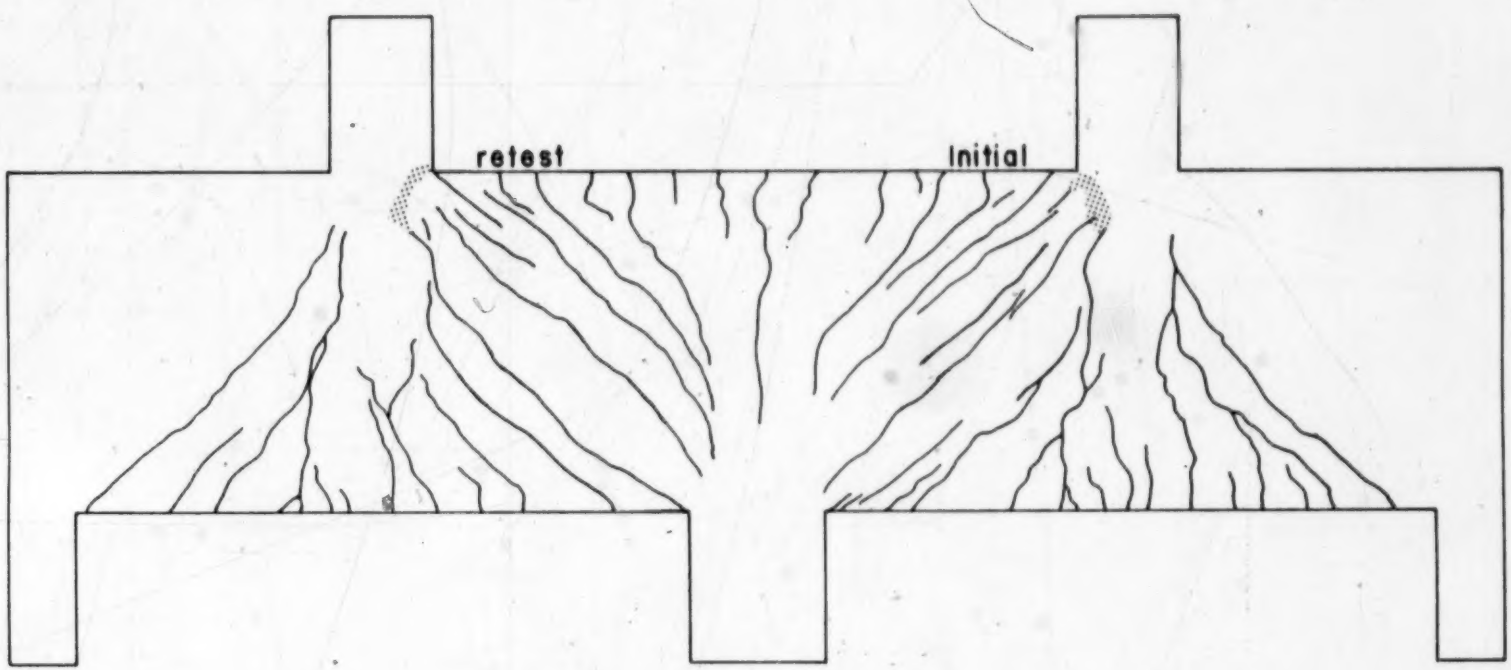

Figure 4.8 Beam 3: Crack Pattern

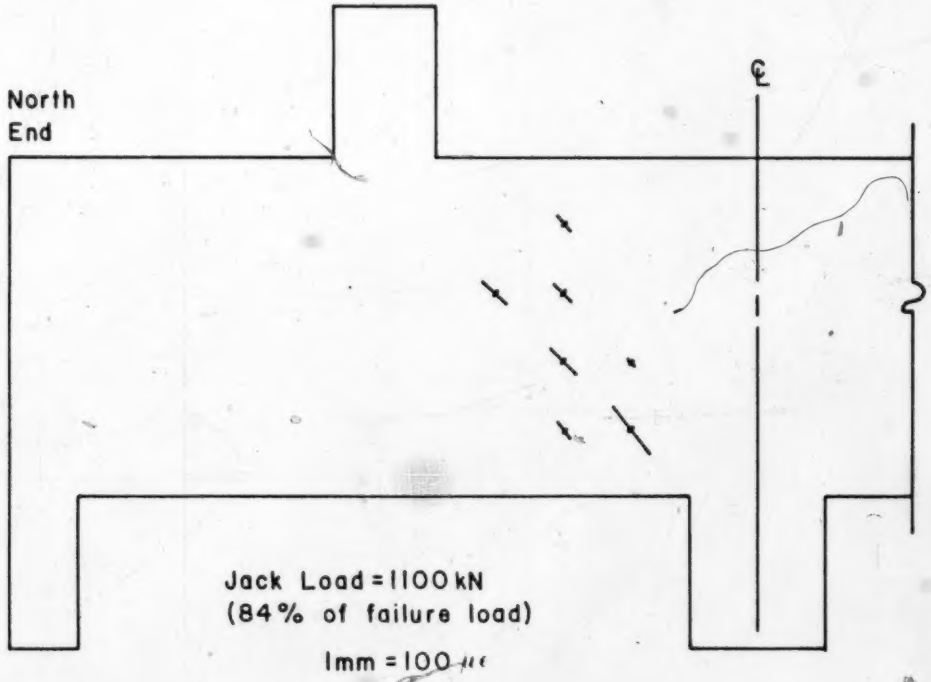

Figure 4.9 Beam 3: Concrete Compressive Strains

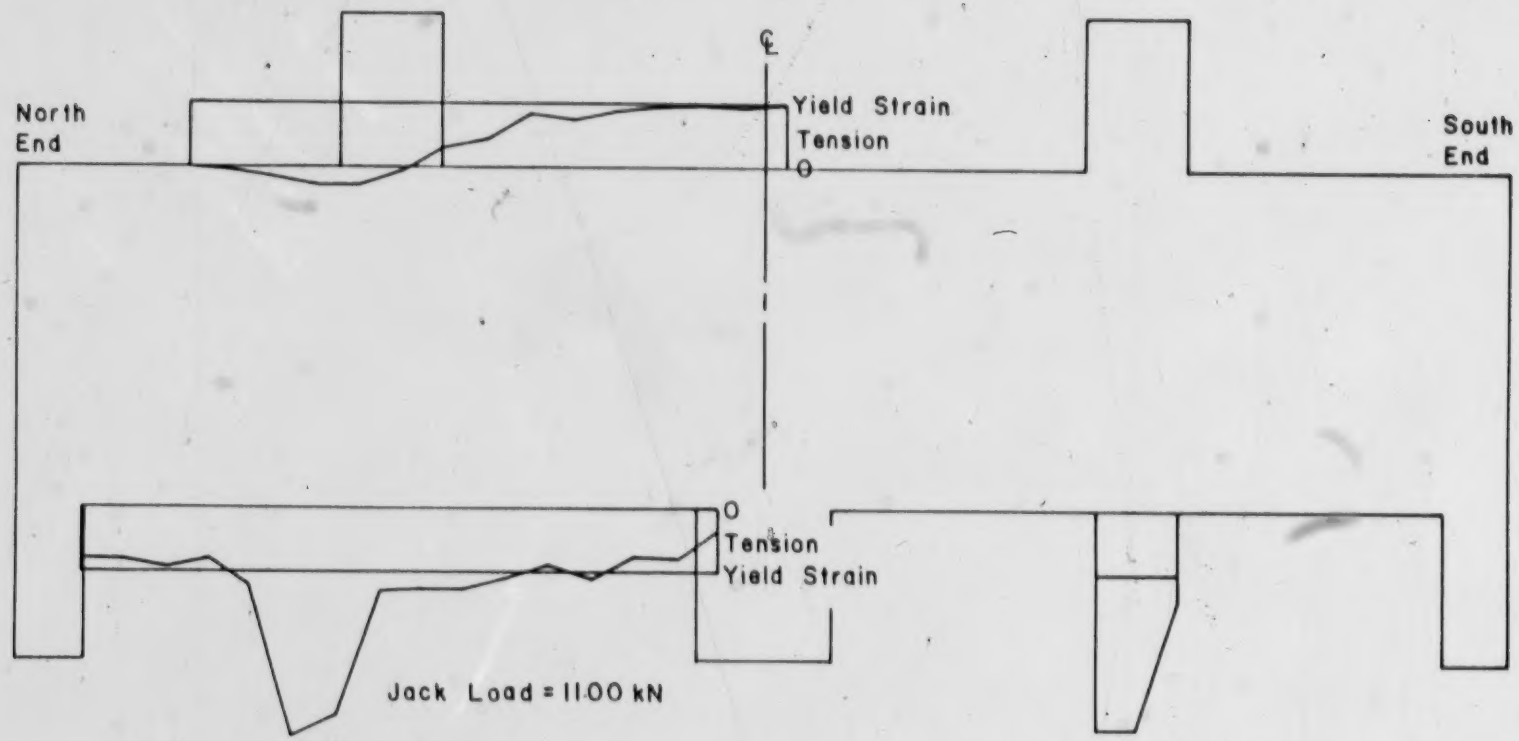

Figure 4.10 Beam 3: Steel Strains

steel. As this failure occurred there was evidence of concrete crushing near the interior support column. During the retest the failure in the south span occurred at a load of about 1570 kN. It appeared to be initiated by the crushing of the direct strut near midhieght in the beam. This was followed by crushing near the load and support columns, and then failure of several of the stirrups at the same locations as described previously. The crack pattern at failure is depicted in Figure 4.11.

The longitudinal reinforcing steel had reached yield in both the bottom and top chords at failure. The bottom chord yielded at a load of about 1200 kN (80% of the failure load), while the top chord did not yield until just before failure, while holding at a load of 1500 kN. All of the stirrups in the interior shear span had yielded at failure. However, the stirrups in the exterior shear span did not yield.

The principal compressive concrete strains are plotted in Figure 4.12 for a jack load of 1200 kN (80% of failure load). The largest such strain was 0.00100. Steel strains are also plotted for this load level in Figure 4.13.

4.4.5 Beam 5

Flexural cracking initially occurred in the positive moment region at a load of approximately 350 kN. In the negative moment region, cracks did not appear until a load of about 500 kN was reached. Small diagonal cracks then

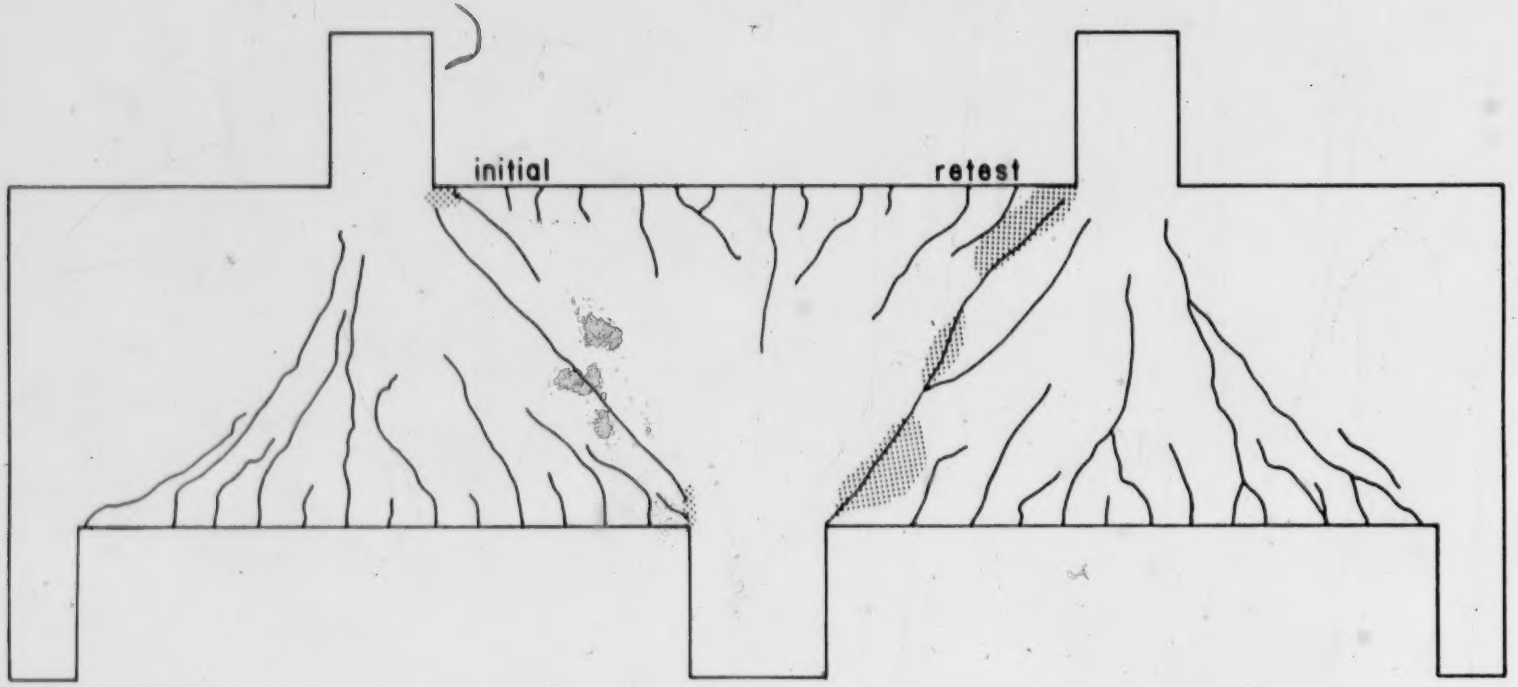

Figure 4.11 Beam 4: Crack Pattern

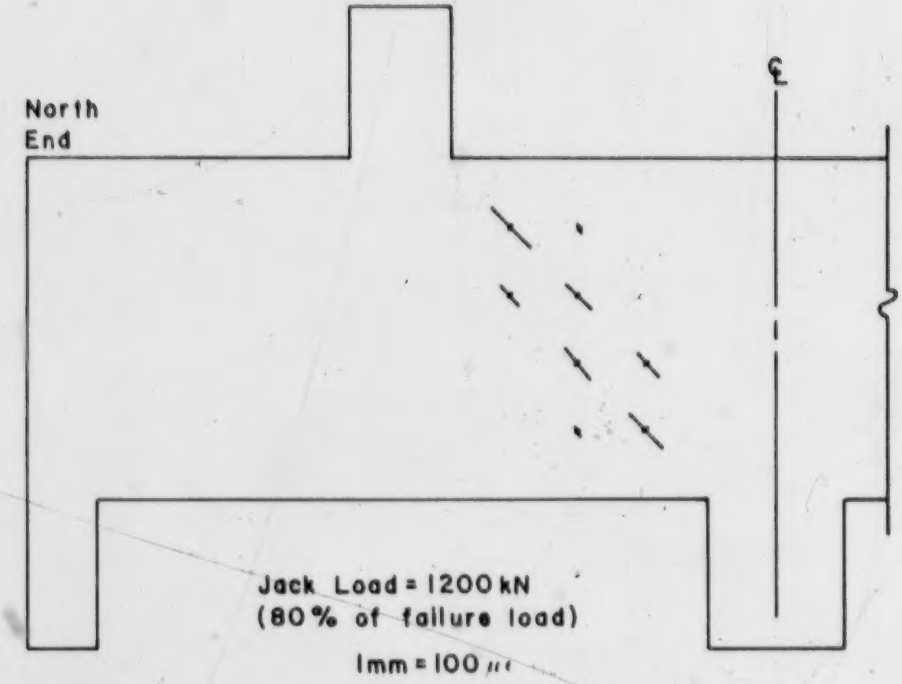

Figure 4.12 Beam 4: Concrete Compressive Strains

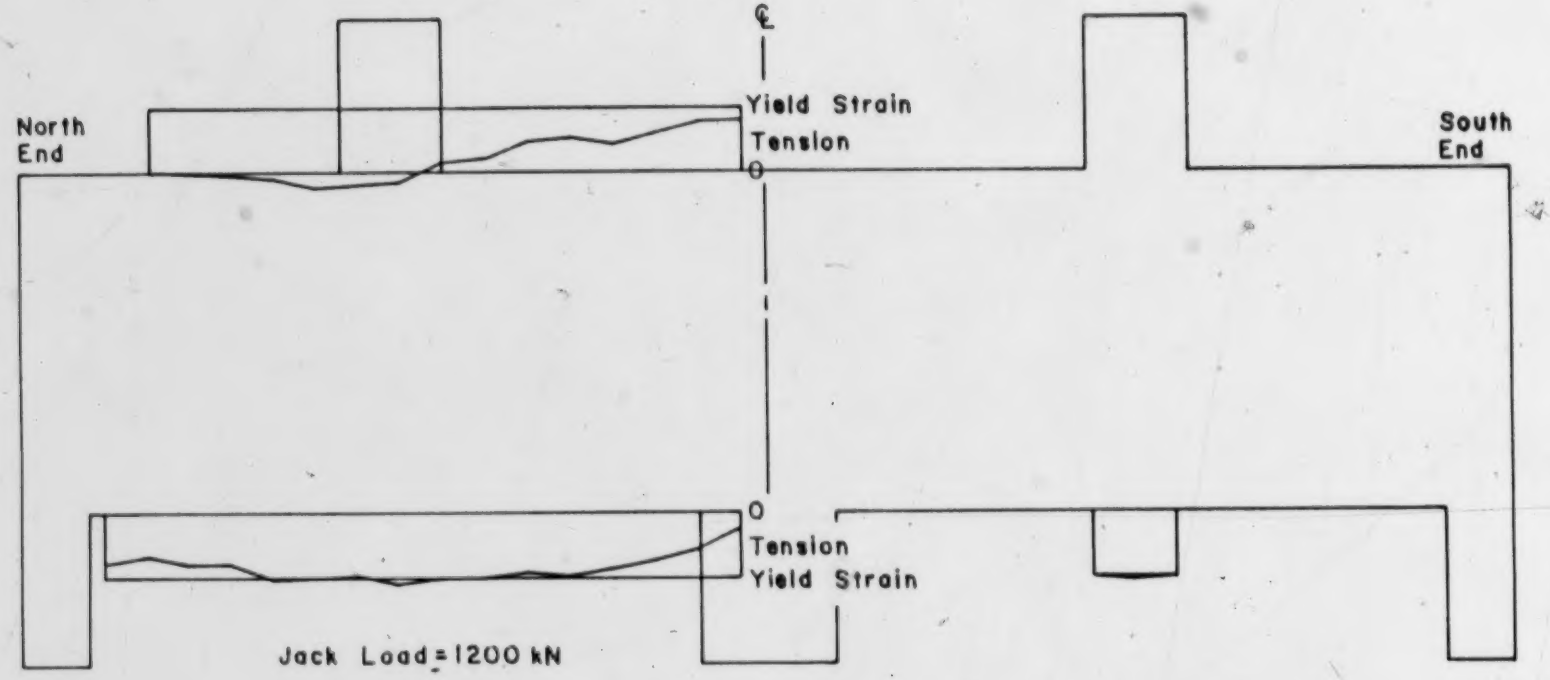

Figure 4.13 Beam 4: Steel Strains

began to appear. In the south interior shear span a large diagonal crack formed with a bang at a load of 700 kN. A similar crack appeared in the north interior span at a load of 1080 kN. The failure commenced with some crushing of the concrete in the direct compression strut at a location about 300 mm away from the load column. The load fell off very gradually to a load of 950 kN over a period of about 30 seconds, at which time the load fell off very rapidly. During the retest, failure occurred in the north interior span at a load of 1300 kN. In this case crushing of the concrete near the load column was visible. Some of the large flexural cracks in the positive moment region had opened to a width of 6 mm as the failure load was reached. The crack pattern at failure is shown in Figure 4.14.

The longitudinal steel reached yield in the bottom chord at a load of about 900 kN (83% of failure load). However, the top chord reached yield just as the beam failed. All of the stirrups in the interior shear spans had yielded at failure, while it appeared that some of the stirrups in the exterior spans did not yield.

The principal compressive concrete strains are plotted in Figure 4.15 for a jack load of 900 kN (83% of the failure load). The largest such strain was 0.00067. Figure 4.16 presents the steel strains, also for this load level.

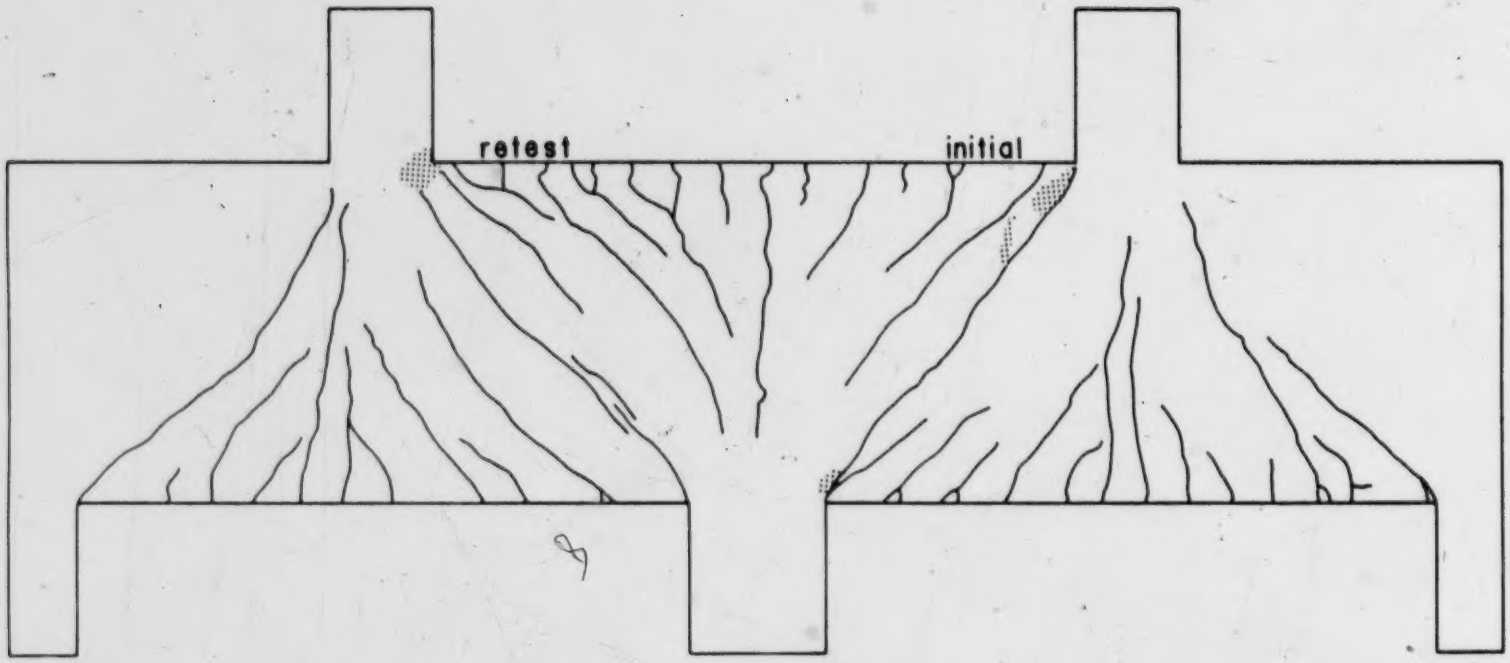

Figure 4.14 Beam 5: Crack Pattern

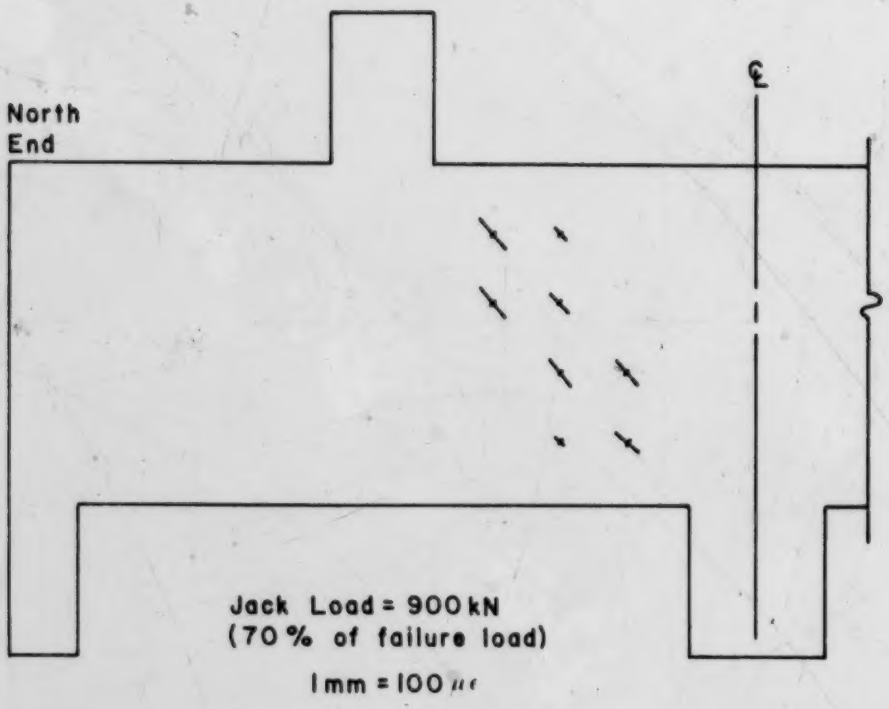

Figure 4.15 Beam 5: Concrete Compressive Strains

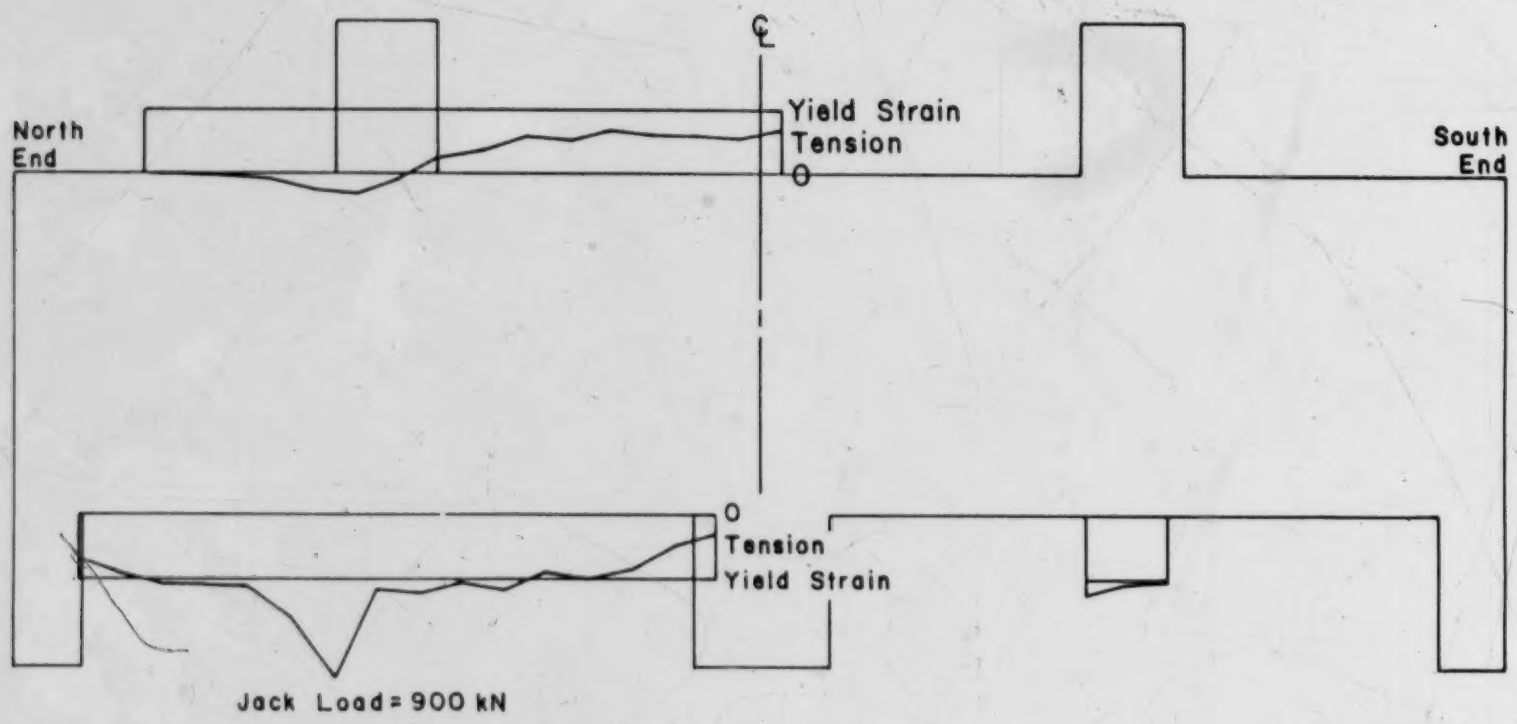

Figure 4.16 Beam 5: Steel Strains

5. INTERPRETATION OF TEST RESULTS

5.1 Truss Models

The application of the plastic truss model outlined in Chapter 2 is demonstrated here for Beam 3 in this test series. This beam has longitudinal steel proportioned roughly in accordance with the elastic bending moment diagram and a 'medium' amount of vertical web steel.

As discussed in Chapter 2, the effective concrete strength $f_c^* = \nu f_c'$ is an important parameter in the truss models. The values of the effectiveness factor, ν, presented in Chapter 2, ranged from about 0.6 to 1.0 for practical concrete strengths and design situations. In Table 5.2 the shear strengths which were calculated using plastic truss models based on ν=0.6 and 1.0 are compared to the measured strengths. The test values lie almost entirely within the range of shear stress values predicted using ν=0.6 and ν=1.0. For the purpose of designing the specimens tested in this study a conservative value of ν=0.6 was used to ensure that the sizes of the truss members would not be governed by concrete cover requirements or the size of the bearing areas. This effective concrete strength was used both in the concrete struts and in the concrete nodal zones. The stress fields shown in Figures 5.1 to 5.5 have all been drawn using ν=0.6. In section 5.2, the values of ν calculated from the state of strain in the concrete are presented.

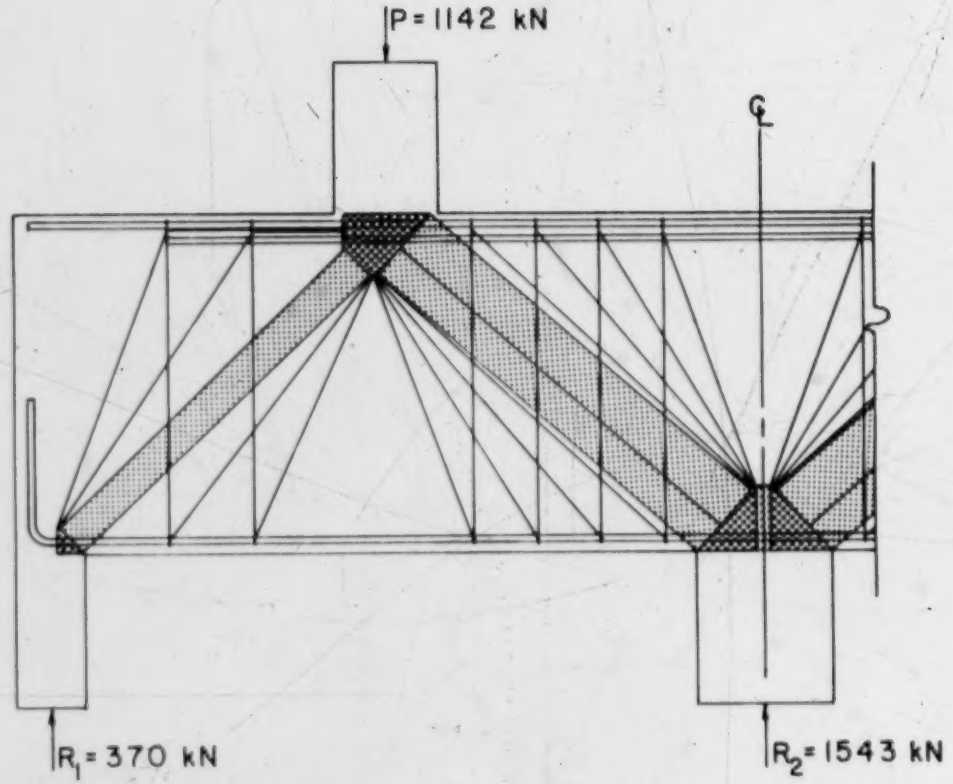

Figure 5.1 Beam 1: Stress Field

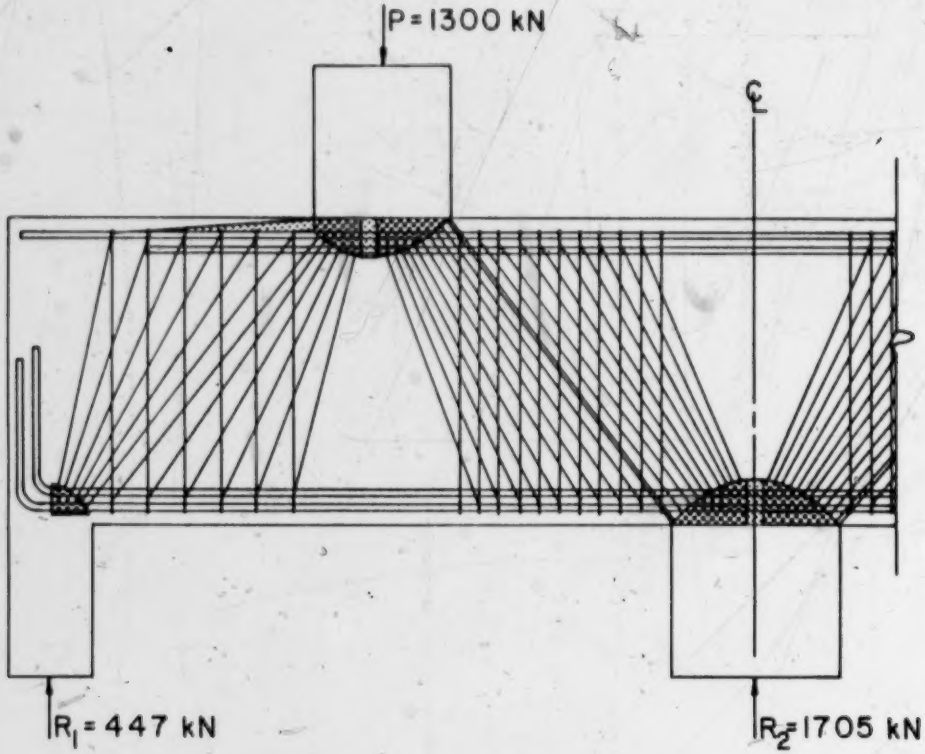

Figure 5.2 Beam 2: Stress Field

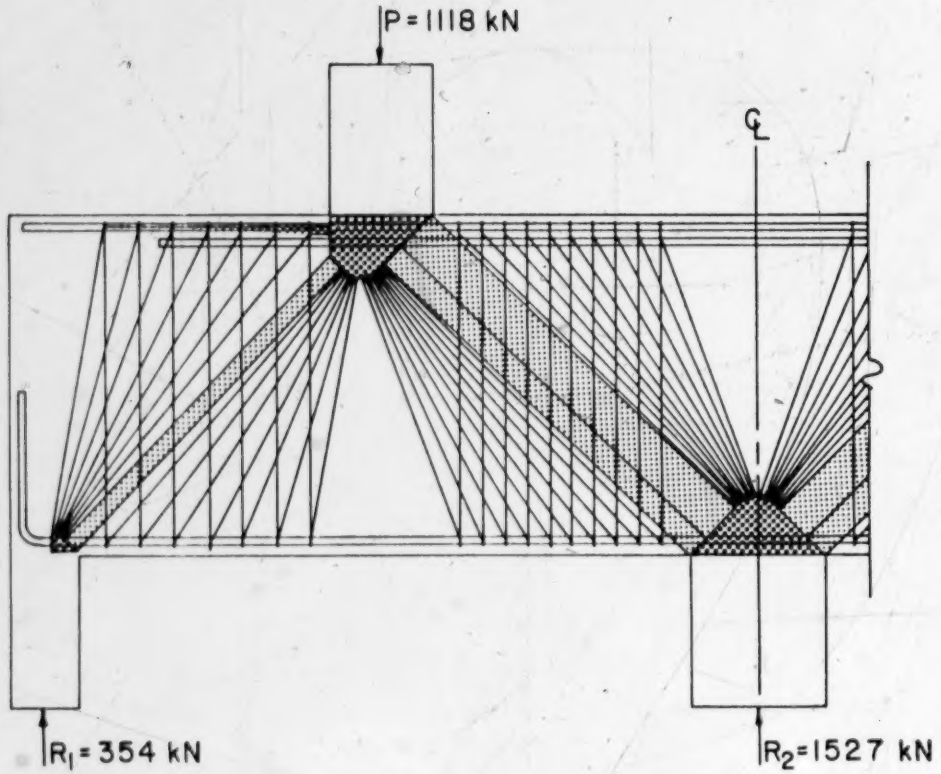

Figure 5.3 Beam 3: Stress Field

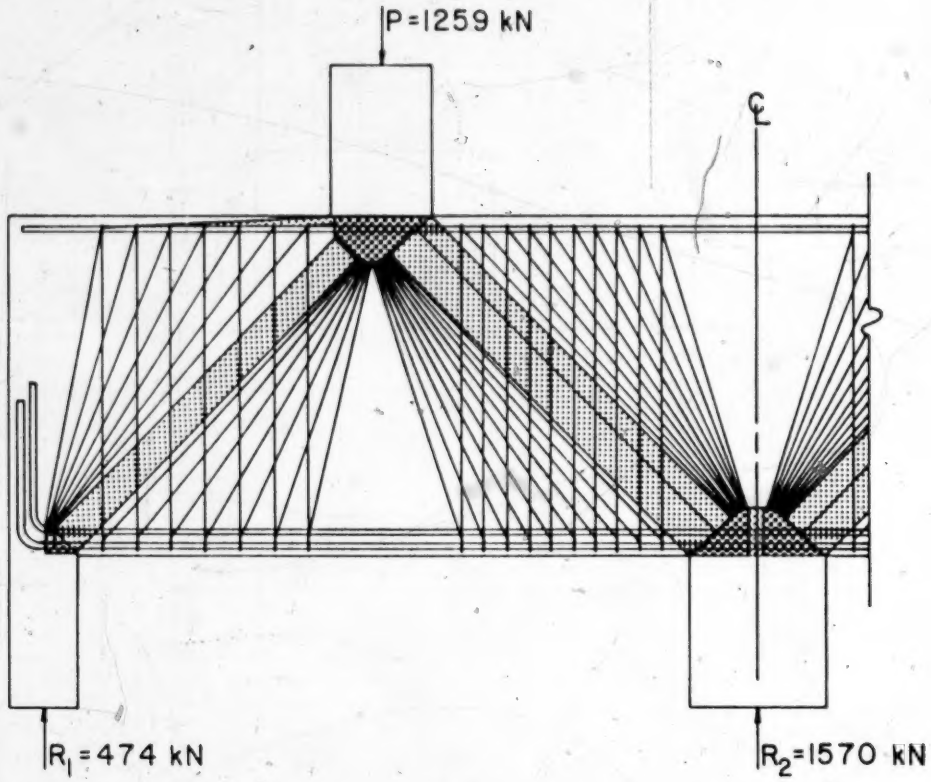

Figure 5.4 Beam 4: Stress Field

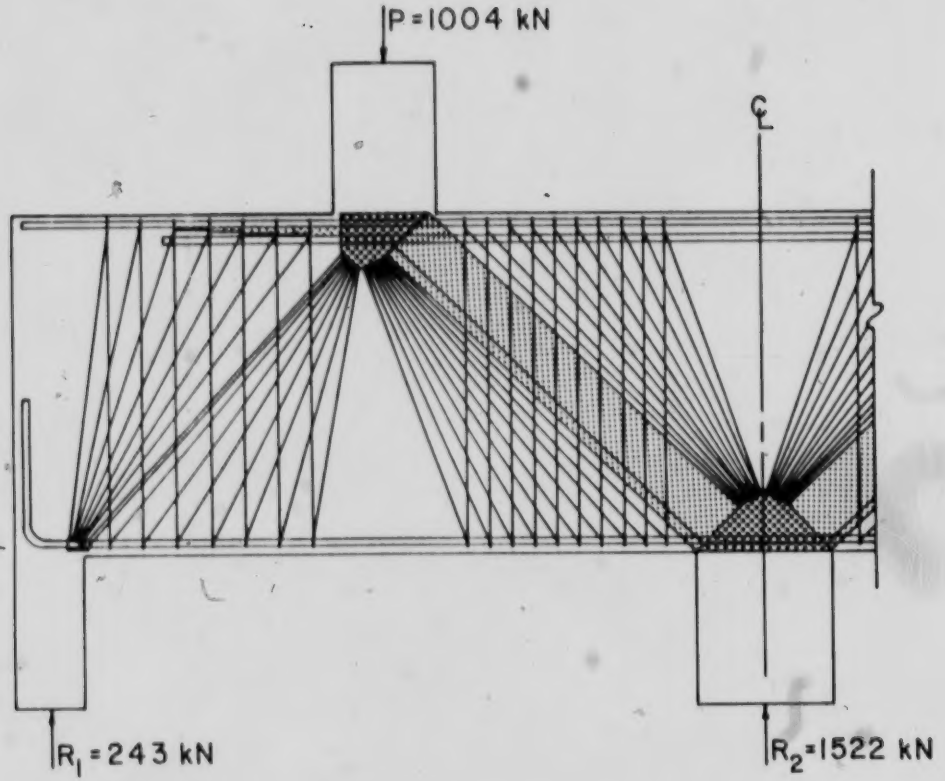

Figure 5.5 Beam 5: Stress Field

Figure 5.3 illustrates an appropriate stress field for one half of Beam 3. The construction of this model is discussed here. Concrete strut members include a series of small radiating struts which connect the load and the reaction points to the intersection of the vertical stirrups and the longitudinal steel. In addition, there are larger direct struts which transfer a portion of the load directly from the loading columns to the reaction columns. In the figures, the struts, which are assumed to be in uniaxial compression, are shown as radial lines or lightly shaded areas and the nodal areas at the intersection of the truss elements are shown in darker shading. The nodal areas are assumed to be in biaxial compression. The widths of the struts are chosen so that the cross sectional area of the strut times the effective concrete strength f_c^*, equals the force in the strut. The struts are drawn to scale in Figures 5.1 to 5.5.

The analysis of Beam 3 shown in Figure 5.3 begins with an initial sketch of the truss from which the member forces can be determined. Normally the truss shown would be statically indeterminate. However, by utilizing the basic assumptions of the plastic truss model presented in Section 2.2.1, the forces in enough steel members can be determined so that the problem is reduced to a statically determinate truss. To accomplish this, the stirrups, the longitudinal steel at midspan and the longitudinal steel above the centre support are assumed to have yielded. By using the 'method of

joints' the remainder of the member forces are then determined, beginning with joints adjacent to known longitudinal steel forces. The top and bottom chord steel forces are reduced at each joint along the length of the chords by the horizontal component of the force in the compression diagonal intersecting at that joint. The force remaining in the chords at the support and loading columns is utilized to equilibrate the direct compression diagonals. Two such diagonals are shown in the interior shear span, one equilibrating the force in the top chord and the other equilibrating the force in the bottom chord. In the case of Beam 3, there is a significant direct strut associated with each of the top and bottom chords. The other beams have either smaller or larger direct struts depending on the amount of steel in the top and bottom chords, the amount of vertical web steel, and the concrete strength.

The reactions and loads which the beam can accommodate are determined by summing the vertical components of all the compression struts which are present at each column.

With this initial analysis complete, the size of all the truss members is recomputed. The geometry can then be refined based on the new strut sizes and the analysis repeated.

The above analysis is only valid if the beam is detailed so that it may accommodate the truss. Therefore, great attention must be paid to the end anchorage of the longitudinal steel, the vertical spacing of longitudinal

steel layers, the concrete cover, and the size of the column bearing areas.

5.2 Calculation of the Effective Concrete Strength from the State of Strain in the Web

As mentioned in Chapter 3, strain measurements were taken on a square grid layout attached directly to the surface of the concrete in an attempt to provide a direct comparison with the test results of Vecchio and Collins (1982). Vecchio and Collins tested large, uniformly strained panels with targets for the strain measurements mounted on the reinforcing steel present in the panels. Strains were measured on an 8 inch grid in such a way that some of the gage lines crossed cracks. Using their results, Vecchio and Collins derived a relationship between the principal tensile strain at failure and the crushing strength of the concrete.

The gage layout in the current test series differs from the Vecchio and Collins layout in that the targets were mounted directly on the surface of the concrete. As with Vecchio and Collins, the six strain measurements for each individual square (see Figure 5.6) resulted in some redundancy in measurement. The 12 different Mohr's circles of strain which can be plotted for each element should be identical, if the six strain measurements are representative of the average state of strain in the element. Vecchio and Collins found this to be close to the case for their test series due to the uniform state of stress in their

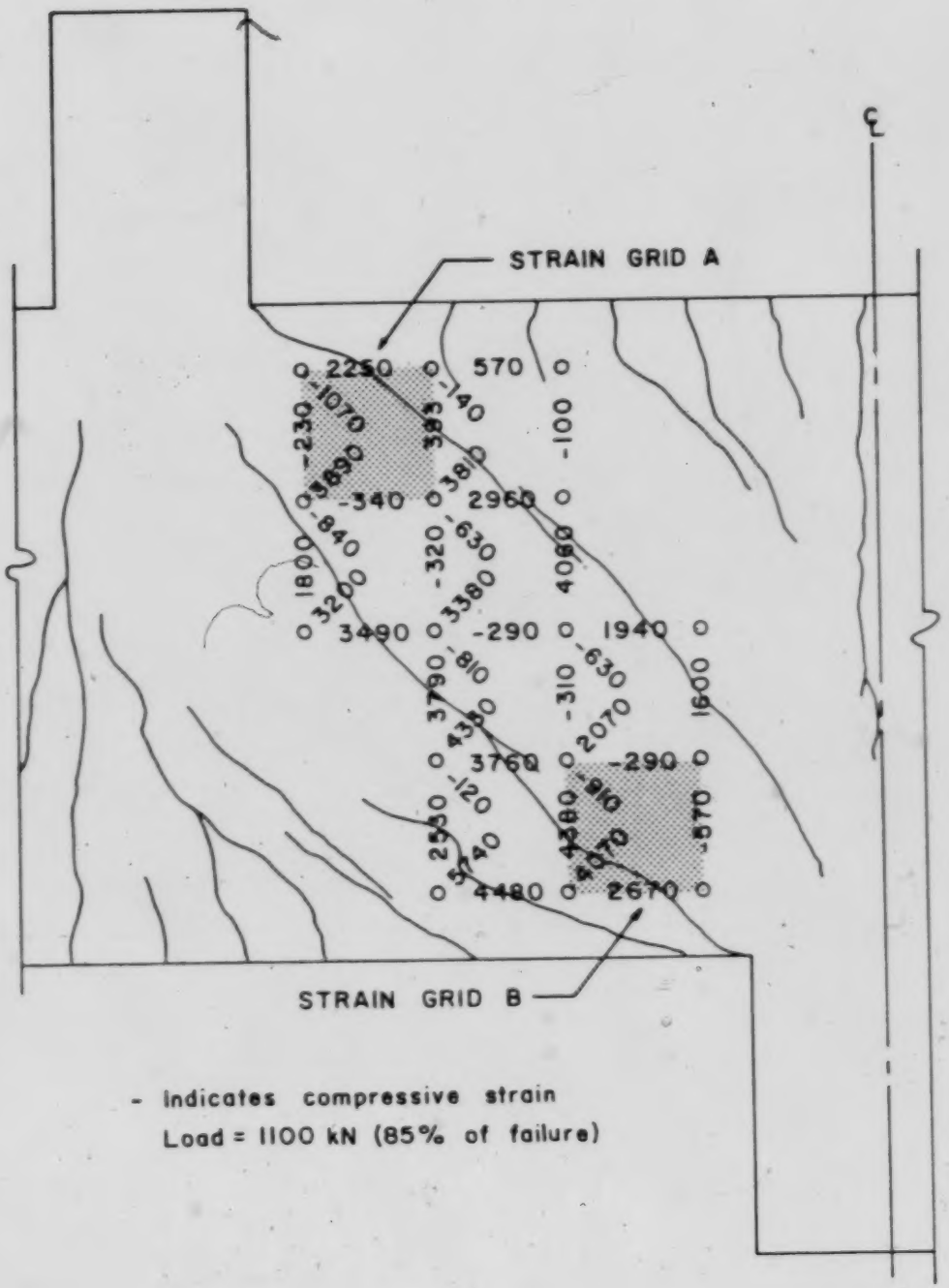

Figure 5.6 Beam I: Concrete Strains

specimens. However, the results of the current series of tests do not corroborate this finding. The target layout, strain readings and crack pattern are shown in Figure 5.6 for an interior shear span of Beam 1. These strain readings were obtained at a load of 100 kN (85% of the failure load in that span). Figures 5.7 and 5.8 show the 12 Mohr's circles of strain for the elements closest to the load column and support column respectively. It is evident from these two figures that the six strain measurements do not adequately represent the state of strain for each element. It appears that the strain field for these beam elements is not the uniform strain field that Vecchio and Collins observed in their tests.

Vecchio and Collins expressed the effective concrete strength as a function of the principal tensile strain ϵ_1 using Equation 2.1:

$$f_c^* = f_c'/(0.8 + 170\epsilon_1) \qquad (2.1)$$

The effective concrete strengths using the ϵ_1 values from the Mohr's circles and Equation 2.1 for strain grid A (Figure 5.7) and strain grid B (Figure 5.8) are given in Table 5.1. These show considerably less scatter than the strain circles would imply. Sixteen of the 24 values in Table 5.1 lie within ± 0.05 of $\nu = 0.64$.

The wide scatter in the values of the principal tensile strain, ϵ_1, suggests that ϵ_1 varies widely in the regions

Table 5.1 Effectiveness factor calculated from the state of strain

Strain Grid A	Strain Grid B
1.12	1.11
.72	.71
.69	.66
.66	.65
.66	.64
.66	.63
.65	.62
.64	.61
.61	.59
.61	.59
.58	.56
.49	.46

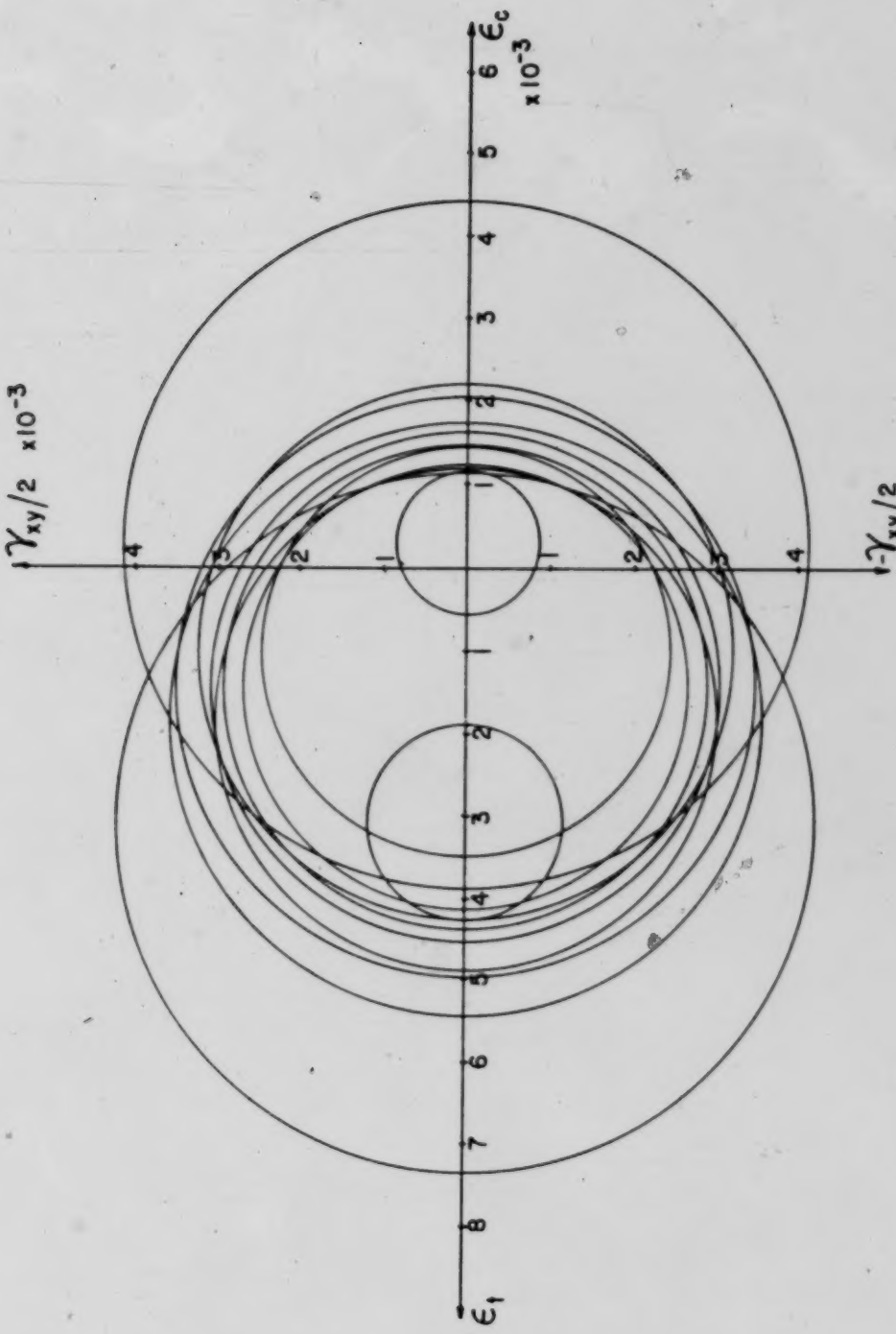

Figure 5.7 Grid A: Mohr's Strain Circles

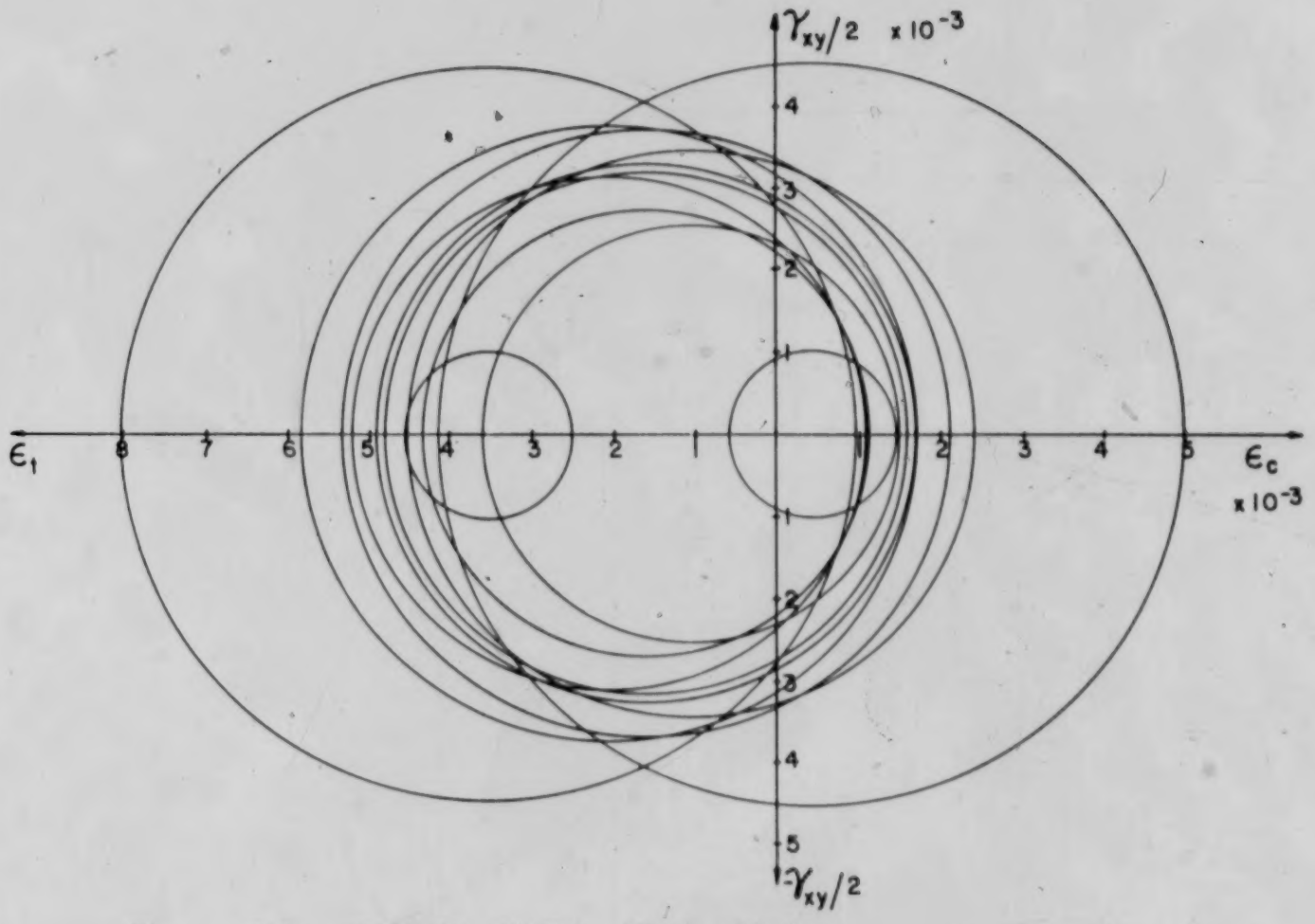

Figure 5.8 Grid B: Mohr's Strain Circles

near the nodal zones at the ends of the direct struts. This finding is of significance since crushing always initiated in these regions.

Clause 11.4.2 of the 1984 Canadian concrete code (CSA, 1984) suggests that ϵ_1 can be calculated using the horizontal strain, ϵ_x, at mid-depth of the beam, which can either be calculated using a plane sections analysis or can be assumed to be equal to 0.002 (tensile). For a deep beam, a plane sections analysis is not appropriate since it does not represent the strut and tie load transfer mechanism. From Figure 5.6 it can be seen that the strains, ϵ_x, at mid-depth, vary from a tensile strain of 0.00349 to a compressive strain of 0.00029 with an average value of 0.00172 (tensile). While this average strain is close to the assumed value of 0.002, it is important to observe that the strain, ϵ_x, where the direct strut crosses the mid-height of the beam, was 0.00029 (compressive). All of these findings suggest that the application of Clause 11.4.2 of the 1984 Canadian code to deep beams warrants more study.

5.3 Ultimate Shear Strengths

The measured and calculated shear strengths are given in Table 5.2. Included in this table are the predicted values based on the plastic truss model, with concrete effectiveness factors ν=0.6 and ν=1.0. In addition, the predicted values according to the American Concrete Institute (ACI) design code ACI 318-83 are included. The ACI

Table 5.2 Ultimate Shear Strengths

Beam		$V_{u\,test}$ (kN)	$\nu = 0.6$		$\nu = 1.0$		ACI	
			$V_{u\,pred}$ (kN)	$\frac{V_{u\,test}}{V_{u\,pred}}$	$V_{u\,pred}$ (kN)	$\frac{V_{u\,test}}{V_{u\,pred}}$	$V_{u\,pred}$ (kN)	$\frac{V_{u\,test}}{V_{u\,pred}}$
1	Initial	754	772	0.98	948	0.80	586	1.29
	Retest	848	772	1.10	948	0.90	586	1.45
2	Initial	948	853	1.11	996	0.95	615	1.54
	Retest	——	——	——	——	——	——	——
3	Initial	836	763	1.10	858	0.97	564	1.48
	Retest	871	763	1.14	858	1.02	564	1.54
4	Initial	926	785	1.18	908	1.02	632	1.47
	Retest	984	785	1.25	908	1.08	632	1.56
5	Initial	774	761	1.02	913	0.85	595	1.30
	Retest	960	761	1.26	913	1.05	595	1.61

predicted values were governed by the upper limits of allowable shear strengths given in Cl. 11.8.3 or Cl 11.8.6. This was due to the fact that the shear to moment ratio at the critical section caused the expression for the concrete contribution to the shear strength in Cl 11.8.6 to 'blow up'. The ratios of the test to predicted strengths indicate that the effective concrete strength used in the plastic truss model lies in the 0.6 to 1.0f_c' range. The test to predicted values for the ACI code indicate that ACI 318-83 is conservative for this a/d ratio. It should be noted that Rogowsky (1983) found the ACI procedure to be conservative for a/d=0.79, but unconservative for larger a/d values in many cases.

In Figure 5.9 the shear stress $v_u = V_u/bd$ is plotted against the web steel percentage times the yield stress, $\rho_v f_y$. Included on this plot are Beams 3/1.0, 5/1.0 and 7/1.0 from Rogowsky's test series, as well as Beams 1, 2 and 3 in the current series. All of these beams have an a/d ratio of approximately 0.79. Both the initial and retest values are plotted. This figure indicates that there is a certain amount of increased shear strength with increased vertical web steel. This increase contradicts Rogowsky's conclusion that for a/d ratios in the range of those plotted, the amount of vertical web steel did not affect the ultimate strength of the beam.

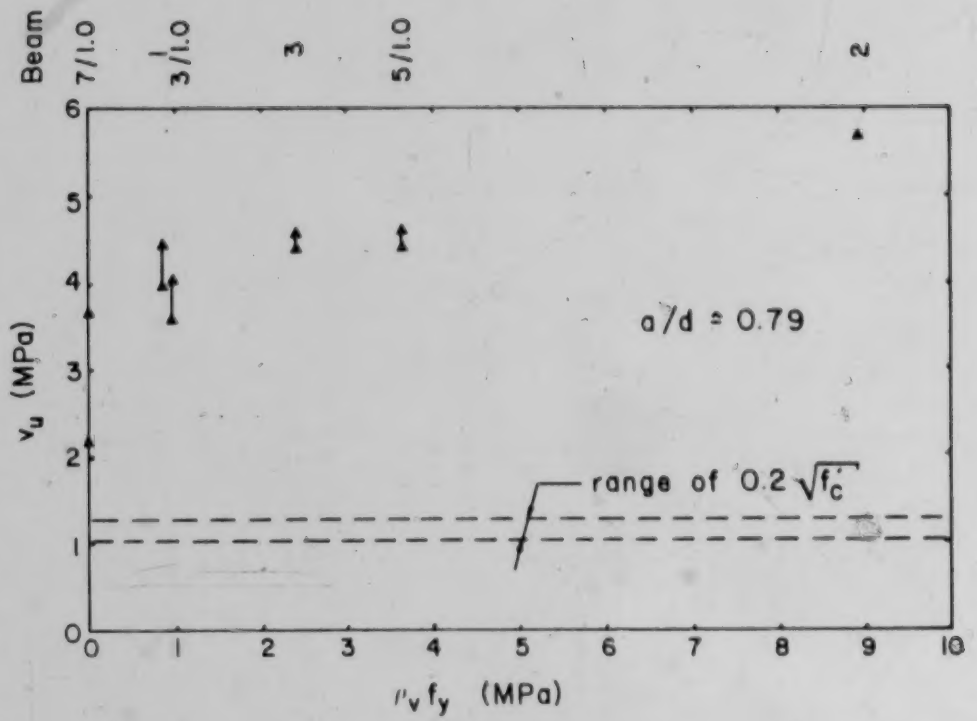

Figure 5.9 Effect of Quantity of Vertical Web Reinforcement

5.4 Distribution of Reactions

The distribution of the reactions is another indication of whether the stress field chosen to model the beam is appropriate. The ratios of reactions to jack loads for the initial tests, retests, the plastic truss predictions and the plastic beam mechanism predictions are given in Table 5.3. For a slender two span beam an elastic analysis would predict $R_2/P=1.375$. As can be seen from the tabulated values the measured reactions were within 3 percent of the predicted values with the exception of the initial tests on Beams 1 and 5. The discrepancy in the initial test of Beam 1 is consistent with the finding that the top chord did not yield in this beam, and therefore the predicted stress field did not fully develop.

5.5 Flexibility of Plastic Truss Model

Beams 3, 4, and 5 had identical web steel and varying amounts of steel in their top and bottom chords. The number of top and bottom bars was 4 and 3, respectively, in Beam 3, corresponding to the elastic distribution of the moments in a slender beam; 3 and 4 in Beam 4; and 5 and 2 in Beam 5. Despite having steel areas which were very different from the elastic distribution of Beam 3, Beams 4 and 5 were both able to redistribute forces within the beam. This redistribution resulted in both the top and bottom chords reaching yield. In each case the bottom steel yielded first and failure occurred almost immediately after the top steel

Table 5.3 Distribution of Reactions at Failure

Beam		R_1/P	R_2/P	R_{2test}/R_{2pred}
1	Initial	.374	1.253	.927
	Retest	.341	1.318	.976
	Predicted*	.324	1.351	
	Rigid Plastic		1.400	
2	Initial	.358	1.285	.979
	Retest	———	———	———
	Predicted*	.344	1.312	
	Rigid Plastic		1.333	
3	Initial	.335	1.330	.974
	Retest	.328	1.342	.982
	Predicted*	.317	1.366	
	Rigid Plastic		1.400	
4	Initial	.380	1.242	.996
	Retest	.372	1.256	1.007
	Predicted*	.377	1.247	
	Rigid Plastic		1.273	
5	Initial	.284	1.432	.945
	Retest	.257	1.486	.980
	Predicted*	.242	1.516	
	Rigid Plastic		1.556	

R_1 = Average of exterior reactions at failure

R_2 = Interior reaction at failure

P = Average of jack loads at failure

* Based on analysis with $r = 0.6$

yielded. This finding suggests that the plastic truss model and the associated stress fields are relatively insensitive to the ratio of $A_{s,t}/A_{s,b}$.

Beam 1, which was identical in most respects to Beam 3/1.0 of Rogowsky's series, was not able to redistribute forces and therefore did not allow the top chord to yield. As with Rogowsky's Beam 3/1.0, the strain in the top chord reinforcement was only 60 to 65% of the yield strain at the time of failure. However both beams failed close to the ultimate loads predicted by the plastic truss model as shown in Table 5.2. In both cases failure occurred by crushing in an interior span near the loading column.

The only significant difference between these two beams, Rogowsky's Beam 5/1.0, and Beam 3 of the current study, was the amount of vertical web steel. Rogowsky's Beam 3/1.0 and Beam 1 contained very little vertical web steel, ρ_v=0.0021 and 0.0018 respectively, while Beam 3 and 5/1.0 had more, ρ_v=0.0052 and 0.0084 respectively. The negative moment steel did not yield in Beam 3/1.0 and Beam 1 but did yield in Beam 5/1.0 and Beam 3. This suggests that the redistribution of forces is dependent on the quantity of web steel.

As predicted by the plastic truss model, the top and bottom chords of Beam 3/1.0 and Beam 1 acted as ties with very little reduction in force along their length. The relatively constant strain profile is illustrated in Figure 4.6. This behaviour resulted in a relatively higher force

remaining in the steel at the support and load columns than for Beam 5/1.0 and Beam 3. Therefore a larger direct compression stut was necessary in Beams 1 and 3/1.0. In addition, the larger steel force in the nodal areas led to a greater strain incompatability between the steel and concrete in the nodal area. This incompatability may have resulted in a premature failure of the concrete in the nodal area due to high local stresses in the concrete.

Another possible explanation for the behaviour of Beam 1 is related to the relative stiffnesses of the webs. A stiffer web should lead to greater redistribution and therefore to the yielding of the top chord. To investigate this hypothesis, an analysis was conducted using a plane truss program (PFT). For comparison purposes, Beams 1 and 3 were analyzed since they were essentially identical except for the quantity of web reinforcement. Initially the member stiffnesses used in the analysis were those predicted by the plastic truss model for each beam. In order to simulate the plastic behaviour of the truss, the analysis was carried out in increments. A load was applied until one member reached its yield force, and then this member's stiffness was significantly reduced for any further load increments.

Following this procedure for the analysis of Beam 3, it was found that the bottom chord reached yield first, followed by the top chord. This is consistent with the test results for this beam. When the failure load predicted by the plastic truss model was reached, the reactions and

distribution of reactions was very close to the predicted values according to the plastic truss analysis and to the test values.

When a similar analysis was conducted on Beam 1 however, the results did not agree with the stress field used in the plastic truss model. While the bottom chord yielded before the failure load was reached, the top chord only reached 90% of its yield stress. When the stiffness of the direct compression struts was adjusted to give the distribution of reactions found in the initial testing of Beam 1, it was found that the PFT analysis predicted that the top chord only reached about 85% of the yield force.

The PFT analysis supports the findings of the test of Beam 1 in which the top chord did not yield. It indicates that a minimum amount of vertical web steel is necessary to allow for the full redistribution of forces within the beam.

Another observation in support of this conclusion is the fact that the chords reached yield at a lower jack load in the retests of Beams 2, 3, 4, and 5 than in the initial tests. This observation indicates that the increased stiffness introduced into the web with the application of the reinforcing yoke has allowed greater redistribution of forces. Unfortunately strain readings were not taken for the top chord of Beam 1 during the retest and therefore the effect of the yoke can not be ascertained for this beam. However, the distribution of reactions for the retest would suggest that greater redistribution of forces did take place.

6. SUMMARY AND CONCLUSIONS

Five two span continuous deep beams were tested to investigate several aspects of deep beam behaviour. All of the beams developed distinctive inclined cracks running from the loading column to the support column. This cracking occurred at loads considerably below the ultimate capacity of the beams. Failure of each of the beams resulted from the crushing of the concrete near the loading or support columns. The top and bottom chords and reached yield when the beams failed in all cases except Beam 1. In this case, only the bottom chord yielded.

The plastic truss model was found to give accurate predictions of ultimate strengths and distribution of reactions. The test values almost all fell within the range of ultimate strength predicted, using an effective concrete strength of $f_c^* = 0.6f_c'$ and $1.0f_c'$.

The calculation of the effectiveness factor, ν, from the state of strain in the concrete as suggested by the Canadian Code, was found not to be appropriate for deep beams. Further research work in this area is thus warranted.

The results of the testing for Beam 1 indicate that a minimum amount of vertical web steel is necessary to allow for the full redistribution of forces within the beam. Further research is needed in order to quantify the amount of vertical web reinforcement required.

The test results for Beam 2 revealed that it was possible to increase the ultimate strength of deep beams

with an increase in the amount of vertical web steel. This finding contradicts Rogowsky's (1983) observation that there is not an increase in shear strength, v_u/f'_c, with a decrease in a/d ratios, for beams with heavy vertical reinforcement.

The results of the tests for Beams 3, 4 and 5 indicate that the plastic truss model is not sensitive to the ratio of $A_{s,t}/A_{s,b}$ and that a suitable stress field can be found for various proportions of top and bottom chord steel provided the beams contain a moderate amount of web steel. The determination of the limits of this flexibility requires further study.

The present research study has examined some aspects of the flexibility of the plastic truss model, and has attempted to further define the limits of the applicability of the model. The plastic truss model gives a visual interpretation of the flow of forces through the beam, as well as providing quantitative information regarding the failure loads and reactions. In conclusion then, the plastic truss model has proven to be a very useful and versatile tool for explaining the ultimate behaviour of deep beams.

REFERENCES

ACI COMMITTEE 318, "Building Code Requirements for Reinforced Concrete (ACI 318-83)", American Concrete Institute, Detroit, Michigan, 1983.

CEB-FIP, "Model Code for Concrete Structures", Information Bulletin No. 124/125E, Paris, France, 1978.

CSA COMMITTEE A23.3, "Design of Concrete Structures for Buildings, CAN3-A23.3-M84", Draft Standard, Canadian Standards Association, Rexdale, Ontario, 1984.

COLLINS, M.P. and MITCHELL, D., "Shear Design by the New Canadian Code", Unpublished paper presented at ACI Conference, Pheonix, Arizona, March, 1984.

GROB, J. and THURLIMANN, B., "Ultimate Strength and Design of Reinforced Concrete Beams under Bending and Shear", Memoires, International Association for Bridge and Structural Engineering, Vol. 36-II, Zurich, 1976, pp. 105-120.

MARTI, P., "Plastic Analysis of Reinforced Conrete Shear Walls", Bericht No. 87, Institut fur Baustatik und Konstruktion, Zurich, November 1978.

NEILSON, M.P., BRAESTRUP, M.W., JENSEN, B.C., and FINN BACH, "Concrete Plasticity, Beam Shear-Shear in Joints-Punching Shear", Special Publication of the Danish Society for Structural Science and Engineering, Technical University of Denmark, Lyngby/Copenhagen, 1978.

RAMIREZ, J., "A Truss Analysis of the Shear and Torsional Strength of Beams", Ph.D. Thesis, University of Texas at Austin, 1984.

ROGOWSKY, D.M., and MACGREGOR, J.G., and ONG, S.Y., "Tests of Reinforced Concrete Deep Beams", Structural Engineering Report No. 109, Dept. of Civil Engineering, University of Alberta, Edmonton, Alberta, 1983.

ROGOWSKY, D.M., and MACGREGOR, J.G., "Shear Strength of Deep Reinforced Concrete Continuous Beams", Structural Engineering Report No. 110, Department of Civil Engineering, University of Alberta, Edmonton, Alberta, 1983.

SCHLAICH, J. and WEISCHEDE, D., "Detailing of Concrete

Structures", Bulletin d'Information No. 150, Comite Euro-International du Breton, Paris, March 1982, pp. 163.

THURLIMANN, B., "Plastic Analysis of Reinforced Concrete Beams", Bericht Nr. 86, Institut fur Baustatik und Kondstruktion, Zurich, November, 1978.

THURLIMANN, B., "Discussion in Session 2", Colloquium on Reinforced Concrete, IABSE Reports of Working Commissions, Vol. 29, Copenhagen, 1979.

THURLIMANN, B., MARTI, P., PRALONG, J., RITZ, P. and ZIMERLI, B., "Anwendung der Plastizitaetstheorie auf Stahlbeton", ("Application of the Theory of Plasticity to Reinforced Concrete"), Institute of Structural Engineering, ETH Zurich, 1983.

VECCHIO, F. and COLLINS, M.P., "The Response of Reinforced Concrete to In-Plane Shear and Normal Stresses", University of Toronto, Dept. of Civil Engineering, Publication No. 82-03, March 1983.